12-1-2019

An optimal allocation and sizing strategy of distributed energy storage systems to improve performance of distribution networks

Choton K. Das
Edith Cowan University

Octavian Bass
Edith Cowan University

Thair S. Mahmoud
Edith Cowan University

Ganesh Kothapalli
Edith Cowan University

Mohammad A. S. Masoum

See next page for additional authors

10.1016/j.est.2019.100847
This is an Author's Accepted Manuscript of: Das, C. K., Bass, O., Mahmoud, T. S., Kothapalli, G., Masoum, M. A.. S., & Mousavi, N. (2019). An optimal allocation and sizing strategy of distributed energy storage systems to improve performance of distribution networks. *Journal of Energy Storage*, *26*, Article 100847. Available here

An optimal allocation and sizing strategy of distributed energy storage systems to improve performance of distribution networks

Choton K. Das[a,*], Octavian Bass[a], Thair S. Mahmoud[a], Ganesh Kothapalli[a], Mohammad A.S. Masoum[b], Navid Mousavi[a]

[a]*School of Engineering, Edith Cowan University (ECU), 270 Joondalup Drive, Joondalup, Perth, WA 6027, Australia*

[b]*Department of Engineering, Utah Valley University, Orem, UT 84058, USA*

Abstract

The allocation of grid-scale energy storage systems (ESSs) can play a significant role in solving distribution network issues and improving overall network performance. This paper presents a strategy for optimal allocation of distributed ESSs through P and Q injection by the ESSs to a distribution network. The investigation is carried out in a renewable-penetrated (wind and solar) medium voltage IEEE-33 bus distribution network for two different scenarios: (1) using a uniform ESS size and (2) using non-uniform ESS sizes. DIgSILENT PowerFactory is used for system modeling and testing, and simulation events are automated using Python scripting. A hybrid meta-heuristic optimization algorithm such as the fitness-scaled chaotic artificial bee colony algorithm is applied to optimize parameters of the objective function. The artificial bee colony algorithm is also applied to justify the results attained from the fitness-scaled chaotic artificial bee colony algorithm. A performance comparison, in relation to proposed PQ injection approach with previously applied P injection technique, is presented. The obtained results suggest that the proposed PQ injection-based ESS placement strategy performs better than the P injection-based approach, which can significantly improve distribution network performance by minimizing voltage deviation, power losses, and line loading.

Keywords: Energy storage system, voltage profile, optimal sizing, power loss, line loading, optimal placement, DER, asset management, network planning, artificial bee colony, DIgSILENT PowerFactory.

Nomenclature

β_{ESS} cost weighting factor in relation to ESSs

β_{LLd} cost weighting factor in relation to line loading

β_{PLs} cost weighting factor in relation to power losses

*Corresponding author

Email addresses: cdas@our.ecu.edu.au (Choton K. Das), o.bass@ecu.edu.au (Octavian Bass), t.mahmoud@ecu.edu.au (Thair S. Mahmoud), g.kothapalli@ecu.edu.au (Ganesh Kothapalli), m.masoum@ieee.org (Mohammad A.S. Masoum), n.mousavi@ecu.edu.au (Navid Mousavi)

Accepted in *Journal of Energy Storage*

β_{VDev} cost weighting factor in relation to voltage deviation

Δt interval of time

η_C charging efficiency of an ESS

η_D discharging efficiency of an ESS

γ_{LLd} cost rate for line loading

γ_{PLs} cost rate for power loss

γ_{VDev} cost rate for voltage deviation

Π^n load weighting factor of bus n

λ^n_{ESS} a variable for representing an ESS position

aP, bP, & cP coefficients for real power of phase a, b, & c

aQ, bQ, & cQ coefficients for reactive power of phase a, b, & c

C^l_{LLd} cost in relation to line loading

C^l_{PLs} cost in relation to power losses

C_{UU} unit cost for UltraBattery

C^n_{VDev} cost in relation to voltage deviation

$E_{ESS-MAX}$ maximum energy of an ESS

$E_{ESS-MIN}$ minimum energy of an ESS

E_{ESS} energy of an ESS

E^{t+1}_{ESS} energy of an ESS at time $t+1$

E^t_{ESS} energy of an ESS at time t

It_{MAX} maximum iteration number in FSCABC optimization

K total number of active ESSs

L_{TRIAL} trial limit to improve a food source in FSCABC optimization

$LB1$ lower limit of decision variable S^n_{ESSP}

$LB2$ lower limit of decision variable S^n_{ESSQ}

$LB3$ lower limit of decision variable λ^n_{ESS}

M total number of lines in the network

N total number of buses in the network

$P_{ESS-MAX}$ maximum power of an ESS

$P_{ESS-MIN}$ minimum power of an ESS

P_{ESS} power of an ESS

$P^D_{i\to k}$ real power delivered from i to a adjacent bus k

P^C_i consumed real power at bus i

P^G_i generated real power at bus i

$P^D_{j\to i}$ power delivered to i from a adjacent bus j

$P^l_{Ls-BASE}$ real power loss without ESS allocation (base case)

P^l_{Ls-ESS} real power loss through optimal ESS allocation

P_{LT} total active power loss

$P_L(i,j)$ active power loss of a line linking two buses, i and j

P_{T-F} input real power (MW) of the feeder

$P^t_{ESS,C}$ charging power of an ESS at time t

$P^t_{ESS,D}$ discharging power of an ESS at time t

P^t_{ESS} power of an ESS at time t

$PF_{ESS-MAX}$ maximum power factor (p.f.) boundary on the dispatch of ESSs

$PF_{ESS-MIN}$ minimum p.f. boundary on the dispatch of ESSs

PF^n_{ESS} p.f. on the dispatch of an ESS on bus n

$PLRI_{P-ESS}$ index for real power loss reduction through optimal ESS allocation

$PLRI_{Q-ESS}$ index for reactive power loss reduction through optimal ESS allocation

$PLRI_{T-ESS}$ index for total power loss reduction through optimal ESS allocation

$Q^D_{i\to k}$ reactive power delivered from i to a adjacent bus k

Q^C_i consumed reactive power at bus i

Q^G_i generated reactive power at bus i

$Q^D_{j\to i}$ reactive power delivered to i from a adjacent bus j

$Q^l_{Ls-BASE}$ reactive power loss without ESS allocation (base case)

Q^l_{Ls-ESS} reactive power loss through optimal ESS allocation

Q_{LT} total reactive power loss

$Q_L(i,j)$ reactive power loss of a line linking two buses, i and j

Q_{T-F} input reactive power (MVar) of the feeder

$R_L(i,j)$ resistance of a line linking two buses, i and j

$S_{ESS-MAX}$ maximum size of an ESS

$S_{ESS-MIN}$ mimimum size of an ESS

S^n_{ESSP} real power (MW) injected by an ESS to nth bus

S^n_{ESSQ} reactive power (MVar) injected by an ESS to nth bus

S_{ESS} size of an ESS in MWh

S^n_{ESS} total size (MVA) of an ESS in nth bus

S^n_{Ld} load at nth bus (p.u.)

S_{PV-MAX} solar DGs' rated capacity (kVA)

S_{PV-OP} solar DGs' operational capacity (kVA)
S_{WIND} wind DGs' total capacity (kVA)
SL^{l-t} loading of lth line
SL^{l}_{BASE} loading of lth line without ESS allocation
SL^{l}_{ESS} loading of lth line after ESS allocation
SL^{l}_{MAX} maximum loading limit of lth line
SL^{l}_{RATED} rated ampacity of lth line
SOC^{x}_{ESS} state of charge of xth ESS
$UB1$ upper limit of decision variable S^{n}_{ESSP}
$UB2$ upper limit of decision variable S^{n}_{ESSQ}
$UB3$ upper limit of decision variable λ^{n}_{ESS}
V^{n-t}_{B} voltage at times t in a day
V^{n}_{B} voltage of nth bus (p.u.)
V_{MAX} upper limit for voltage
V_{MIN} lower limit for voltage
V_{RATED} system's rated voltage (p.u.)
V_{REF} reference bus voltage (p.u.)
V_{Target} system's target voltage
$X_L(i,j)$ reactance of a line linking two buses, i and j
X_{TLLoss} Total line loss
% LLd^{l}_{BASE} percent loading of lth line without ESS allocation
% LLd^{l}_{ESS} percent loading of lth line after ESS allocation
% $LLdT_{w-ESS}$ total percent loading of a line after ESS allocation
% $LLdT_{wo-ESS}$ total percent loading of a line without ESS allocation

1. Introduction

Today's power systems encounter a period of change originated by various issues in relation to energy crisis and renewable integration [1–4], demand management and appropriate use of energy [5–8], greenhouse gas (GHG) emissions [9, 10], voltage profile and power quality management [11, 12], network congestion management [13], power system reliability [14, 15], and network expansion [16]. Energy storage systems (ESSs) are growingly being integrated in distribution networks to offer various advantages related to technical, economic, and environmental issues [17, 18]. These encompass facilitating renewable energy source (RES) integration [19–21], power compensation [22, 23], load levelling [24] and peak shaving [25], load shifting [26, 27], frequency regulation [28, 29], voltage control or mitigation of voltage deviation [30, 31], power quality improvement [28, 32], RES energy time-shifting [33] and distributed generation planning [34], energy arbitrage [35] and operating reserves [36, 37], network expansion [38], overall cost reduction [39] and profit maximization [28, 40], greenhouse gas (GHG) reduction [41, 42], and network reliability [43, 44]. However, the benefits from the ESS placement cannot be achieved in cases of their misuse or misplacement in distribution networks [45].

Asset management in distribution networks is considered as a vital task by network service providers for ensuring reliable network operation. However, this can be an expensive task which might increase network cost, such as the cost due to network reinforcement for voltage and thermal stability. Consequently, electricity prices can be affected significantly. Therefore, providing a low cost solution to distribution network operators targeting a better asset management practice is the motivation of this work. Optimal allocation of ESSs, based on performance expectations and optimization approaches, is reported in several studies [28, 31, 32, 38, 43, 46–63].

A comprehensive review on ESS placement, sizing, and operation is presented in [17] for mitigating the issues of distribution networks. This study also presents the role of ESSs for power quality improvement. In [46], an optimal allocation of ESSs is performed in an IEEE-33 bus distribution network to minimize voltage deviation, line losses, and line loading. In that paper, the ESS sizing is accomplished through the application of a unity power factor (p.f.) approach on the dispatch of ESSs, where the ESSs only inject P to the network. Ref. [38] proposes an optimal placement of distributed community-based ESSs in distribution networks to achieve the benefits from energy loss reduction, energy arbitrage, peaking photovoltaic (PV) generation, emission reduction, network upgrade deferral, and Var support. This study demonstrates that load models should be incorporated in an ESS planning problem to obtain more realistic outcomes, while applying the constant power load model may miscalculate the profitability of ESS investment.

An optimal placement and sizing of ESSs, for improving voltage profile of a wind-penetrated distribution system and minimizing cost of the system, is accomplished in [47]. In [48], the planning and control of ESSs is performed in an RES-integrated distribution network to minimize operational and investment costs, while focusing on a network of static ESSs accompanied by deterministic capacity. In [49], the risk of energy transaction mechanisms for energy agents under a distribution company is mitigated through optimal ESS placement. In this study, two types of ESS technologies such as Lead-acid and Li-ion are considered, where interaction among the ESSs is performed through the achievement of Nash equilibrium. However, other performance indices such as improvements of voltage profile and power quality are not investigated. In [50], ESS allocation is optimized for the risk mitigation of distribution companies while reducing operational costs and maximizing energy transaction profits. This study also considers Lead-acid and Li-ion ESS technologies for investigation and does not include voltage profile improvement or line loading minimization in the objective function. Total energy loss of a distribution network is minimized by optimal ESS placement and sizing in [51]. This study demonstrates some limitations and indicates possibilities for future research including development of further realistic models, thorough mathematical modeling of radial networks, and further investigations on background injections at buses considering complicated spatial structure. In [28], the net profit of distributed ESSs is maximized through the achievement of energy reserve and energy price arbitrage, distribution system congestion management, and a frequency regulation service through controlling active and reactive powers. This study also presents the importance of reactive power control to simultaneously support efficient energy trading and balancing services, and network congestion management.

In [52], the ESS placement is accomplished for both distribution and transmission networks. The optimal ESS size on the distribution side is calculated to address peak load shaving and load curve smoothing. On transmission side, a sensitivity analysis is performed using a time domain power flow, complex-valued neural networks, and economic dispatch to place the ESSs. Ref [53] investigates the impact of ESS configuration and location on voltage profiles, power losses, and utilization of ESSs within a feeder of a low voltage (LV) distribution network. This research also suggests that either a power electronic system without ESSs or a single-phase ESS may be deployed to attain cost-effectiveness of the

system. In [31], a multi-objective optimal ESS allocation and sizing problem is formulated to mitigate voltage deviations and improve supply quality, eliminate line congestions and load curtailment, and minimize electricity and distribution network costs. An optimal ESS allocation strategy is proposed in [55] to simultaneously minimize voltage deviation, operation cost, and air emission of a wind-penetrated power system. However, this study did not consider line loading and losses during objective function formulation. In [54], an optimal ESS management strategy is proposed for an RES-penetrated distribution system to minimize energy losses of the network, GHG emissions, and overall power generation cost. This paper indicates some future research opportunities such as- (i) identifying sensitive network branches and adjusting sections to reduce energy losses and (ii) identifying and installing the most appropriate ESS technology.

In [57], optimal allocation and operation are performed for distributed ESSs for improving load and generation hosting capability. As a result, peak demand and power loss are reduced achieving better voltage regulation. In [58], optimal ESS allocation in an LV distribution network is performed targeting the prevention of under- and over-voltages and minimization of total network costs (regarding ESS and network losses). This research did not investigate minimization of line loading and application impact of optimal ESS control algorithms in real-time network operation scenarios. In [59] and [60], the ESS allocation is performed for minimizing the problem of voltage fluctuations due to PV integrations in LV networks, while not investigating RES integration impact on line losses and loading. Again in [32], the allocation of distributed ESSs is performed for minimizing both network losses and the energy cost in relation to congestion management and external grid, and for providing voltage support.

In [61], optimal ESS allocation is accomplished to maximize distribution network benefits through minimizing the costs of ESS installation, energy losses, maintenance, interruption, and system upgrade. In [56], optimal ESS placement and sizing are accomplished for maximizing distribution system benefits while managing loads, and minimizing total costs and net present value (NPV). Both studies [61] and [56] consider three ESS technologies, e.g., Lead-acid, vanadium redox (VR), and sodium sulfur (NaS) for performance comparison. However, these studies did not investigate improvement of voltage profiles and distribution system reliability. In [62], a planning framework is developed for determining optimal location and sizes of distributed ESSs in wind-penetrated power systems to minimize costs in relation to wind curtailment and line congestion, and to maximize the normalized profit of ESS owners. In [43], optimal ESS placement is performed to minimize interruption and annual costs as well as improve reliability of distribution systems. In [63], the annual electricity cost is minimized through optimal ESS allocation in a wind-penetrated distribution network, where reliability enhancement and peak shaving are not considered.

In the above literature, various optimization and modeling techniques (single and hybrid) are employed for the optimal allocation of ESSs [28, 31, 32, 38, 43, 46–63]. In [46], the artificial bee colony (ABC) algorithm is applied for optimal ESS allocation in distribution networks and the results are verified through the application of the particle swarm optimization (PSO) approach. A probabilistic load flow, a hybrid multi-objective PSO integrating a non-dominated sorting genetic algorithm (NSGA-II), and a five-point estimation method

(5PEM) technique are used in [47]. Again, a fuzzy PSO (FPSO) is utilized in [50]. An optimal power flow (OPF) with mathematical modeling technique is applied in [51]. A multi-agent approach based on game theory is employed in [49]. Ref. [31] uses the AC-OPF and mixed-integer second order cone programming (MISOCP) approaches for optimal placement of ESSs. A mixed-integer linear programming (MILP) approach is applied for optimal ESS placement in [28], while [48] presents a network-aware technique for the planning and control of ESSs. In [54] and [62], the NSGA-II is used for optimization, while [55] employs two multi-objective approaches such as gravity search algorithm and a hybrid PSO-GA algorithm for optimization. Ref. [59] applies a genetic algorithm (GA)-based technique combined with simulated annealing, while [60] applies a GA-based bi-level optimization strategy for solving optimal ESS placement problem. Again in [32], an alternating direction technique to multipliers is employed for the placement of distributed ESSs. In [58], clustering and sensitivity analysis and the multi-period OPF approaches are applied. The GA (integrated with linear-programming) and a sequential Monte Carlo simulation (MCS) are used in [43, 61], while these strategies along with MATLAB optimization toolbox are employed in [56]. A multi-objective optimization technique (cost-based) by MATLAB is used in [57]. However, the application of hybrid optimization algorithms is also recommended in [17, 64, 65] for obtaining good optimal solutions.

This paper introduces a hybrid optimization technique, namely a fitness scaled chaotic artificial bee colony (FSCABC) algorithm [66, 67] for optimal placement of ESSs. Being simple and robust, the ABC algorithm has triple search capability to solve complex combinatorial and multi-dimensional optimization problems [46, 68–70]. The hybrid FSCABC technique improves the performance of ABC algorithm by eliminating the trapping problem in local optima [66, 67, 71]. Although various issues of distribution networks are addressed in the aforementioned literature, very few studies ([46]) simultaneously focus on voltage profile improvement, line loading minimization, and power loss reduction. Moreover, the investigations for optimal ESS placement are carried out in [46] injecting P only (Q=0) from the ESSs to the network. However, the performance can be improved further with P and Q injection by the ESSs. This paper has addressed this need.

In this paper, an optimal placement problem of distributed ESSs, in an IEEE-33 bus distribution network, is investigated and formulated. DIgSILENT PowerFactory is used for system modeling and analysis, and the FSCABC optimization technique is employed for optimization. Python programming language is utilized for controlling the models developed in PowerFactory and facilitate optimization. The key contributions of this paper are outlined as follows:

- The investigation for optimal allocation of ESSs is carried out focusing on voltage profile improvement, line loading reduction, power loss minimization (real and reactive), and ultimately cost minimization. The optimal ESS allocation related research such as [32, 47, 53–55, 58, 62] have not widely considered these parameters together except [46]. Although similar investigation is carried out in [46], a unity p.f. approach is applied on the ESS dispatch (i.e. the ESSs only inject P to the network). In this study, however, the ESSs inject both the P and Q to the network for better performance improvement with variable p.f. on the dispatch of an ESS.

- The ESSs are placed in the networks by two different approaches: (1) using a uniform ESS size, and (2) using non-uniform ESS sizes. These sort of approaches have not been utilized by earlier studies such as [31, 32, 49, 50, 53, 57, 63] except [46]. The results obtained by using these approaches are analyzed and compared with [46] which establishes the performance improvement. Although the FSCABC optimization technique is applied for these investigations, ABC algorithm is also utilized to verify the results attained from the FSCABC approach.
- The performance indices are estimated to monitor the performance improvement after optimal ESS placement in the network, which are not estimated by the related studies except [46].

The structure of this paper is organized as follows: The modeling of ESSs is presented in Section 2. Section 3 discuses the formulation of the problem, while the optimization and proposed approaches are presented in Section 4. Section 5 discusses about the test network, factor assignment, and performance indices. The results are analyzed, compared, and discussed in Section 6. The paper concludes with remarks and future research directions in Section 7.

2. Modeling of the ESS

The selection of utility-scale ESSs relies upon various performance factors, technical characteristics, and applications [17, 72]. Similar to [46], the UltraBattery (also called advanced lead-acid battery) is selected in this research from the viewpoint of ESS cost. Although the UltraBattery is selected as the ESS technology, the proposed ESS model is taken into account as generic and can be utilized for other ESS technologies.

The ESS model is subjects to the following constraints:

- The ESS is fully charged if state of charge $SOC^x_{ESS} = 1$ and fully discharged if $SOC^x_{ESS} = 0$.
- The ESS should control the real power in both ways and the SOC^x_{ESS} is subject to the following constraint [73]:

$$0.2 \leqslant SOC^x_{ESS} \leqslant 0.9 \tag{1}$$

- A priority for real and reactive powers (P and Q) is required to satisfy the rated apparent power $S_{APP} = \sqrt{P^2 + Q^2}$.

In addition, the ESS should satisfy boundary conditions from (2) to (7) in time t (indexed $1, ..., NT$) [46]. The charging and discharging powers are estimated through (2) and (3), respectively [46]. Restrictions on energy stored by the ESS and ESS charging power are applied by (4) and (5), respectively. Furthermore, the constraints for energy released from

the ESS and power discharged by the ESS are defined by (6) and (7), respectively [46].

$$P^t_{ESS,C} = max\{P_{ESS-MIN}, \frac{(E^t_{ESS} - S_{ESS-MAX})}{\eta_C \,.\, \Delta t}\} \tag{2}$$

$$P^t_{ESS,D} = min\{P_{ESS-MAX}, \frac{(E^t_{ESS} - S_{ESS-MIN})\,\eta_D}{\Delta t}\} \tag{3}$$

Charging mode:

$$E^{t+1}_{ESS} = min\{\left(E^t_{ESS} - \Delta t\ P^t_{ESS,C}\ \eta_C\right),\ S_{ESS-MAX}\} \tag{4}$$

$$P^t_{ESS,C} \leqslant P^t_{ESS} \leqslant P^t_{ESS,D} \tag{5}$$

Discharging mode:

$$E^{t+1}_{ESS} = max\{\left(E^t_{ESS} - \Delta t\ \frac{P^t_{ESS,D}}{\eta_D}\right),\ S_{ESS-MIN}\} \tag{6}$$

$$P^t_{ESS,C} \leqslant P^t_{ESS} \leqslant P^t_{ESS,D} \tag{7}$$

3. Formulation of the problem

3.1 Objective function

The objective function of the proposed optimal ESS allocation problem is given in (8) and formulated using (9) to (16) [46]. This is a cost function which includes the costs in relation to network performance such as voltage deviation, line loading, and line losses as well as ESS units [46]. Of note, equation (8) is not a multi-objective function as formulated in [74] where a Pareto front is used to determine an optimal solution amongst multiple solutions. This function comprises the performance cost factors (C^n_{VDev}, C^l_{LLd}, and C^l_{PLs}) as well as ESS cost factor (C^{UTo}_{ESS}) which are weighted equally with β_{VDev}=β_{LLd}=β_{PLs}=β_{ESS}=1.

$$\mathcal{J}(C_{Fi}) = minimize\left\{\underbrace{\left(\beta_{VDev}\cdot C^n_{VDev} + \beta_{LLd}\cdot C^l_{LLd} + \beta_{PLs}\cdot C^l_{PLs}\right)}_{C_{performance}} + \left(\beta_{ESS}\cdot\ C^{UTo}_{ESS}\right)\right\} \tag{8}$$

where,

$$C^n_{VDev} = \left(\sum_{n=1}^{N} |V_{Target} - V^n_B(S^n_{ESSP}, S^n_{ESSQ}, \lambda^n_{ESS})|\right)\cdot\ \gamma_{VDev} \tag{9}$$

$$C^l_{LLd} = \left(\sum_{l=1}^{M} \%\ LLd^l_{ESS}(S^n_{ESSP}, S^n_{ESSQ}, \lambda^n_{ESS})\ \right)\cdot \gamma_{LLd} \tag{10}$$

$$\%\ LLd^l_{ESS}(S^n_{ESSP}, S^n_{ESSQ}, \lambda^n_{ESS}) = \left(\frac{SL^l_{ESS}}{SL^l_{RATED}}\right) \times 100 \tag{11}$$

$$C_{PLs}^{l} = X_{TLLoss} \cdot \gamma_{PLs} \tag{12}$$

$$X_{TLLoss} = \sqrt{\left\{P_{LT}(S_{ESSP}^{n}, S_{ESSQ}^{n}, \lambda_{ESS}^{n})\right\}^{2} + \left\{Q_{LT}(S_{ESSP}^{n}, S_{ESSQ}^{n}, \lambda_{ESS}^{n})\right\}^{2}} \tag{13}$$

$$P_{LT}(S_{ESSP}^{n}, S_{ESSQ}^{n}, \lambda_{ESS}^{n}) = \sum_{l=1}^{M} P_L(i,j) \; = \sum_{l=1}^{M} \left(R_L(i,j) \; \cdot \frac{P_i^2 + Q_i^2}{\left| \left\{ V_B^n(S_{ESSP}^{n}, S_{ESSQ}^{n}, \lambda_{ESS}^{n}) \right\}^2 \right|} \right) \tag{14}$$

$$Q_{LT}(S_{ESSP}^{n}, S_{ESSQ}^{n}, \lambda_{ESS}^{n}) = \sum_{l=1}^{M} Q_L(i,j) \; = \sum_{l=1}^{M} \left(X_L(i,j) \; \cdot \frac{P_i^2 + Q_i^2}{\left| \left\{ V_B^n(S_{ESSP}^{n}, S_{ESSQ}^{n}, \lambda_{ESS}^{n}) \right\}^2 \right|} \right) \tag{15}$$

The total ESS unit cost is estimated by (16) [46]:.

$$C_{ESS}^{UTo} = \sum_{n=1}^{K} S_{ESS}^{n} \cdot C_{UU} \tag{16}$$

In the above-mentioned equations, γ_{VDev} = \$0.142 p.u. [46, 57], γ_{LLd} = \$0.503 p.u. [46, 75], γ_{PLs} = \$0.265 /kWh [46, 75], and V_{Target} = 1 p.u.. Additionaly, C_{UU} = \$460 /kWh considering UltraBattery applications in relation to industrial and commercial energy management [46, 76].

3.2 Constraints of the objective function

The objective function presented in (8) is subject to (17) to (27) including ESS modeling related equations (1) to (7) [46]:

$$P_i^G + \sum_{j \in J+} \left(P_{j \to i}^D\right) = P_i^C + \sum_{k \in J-} \left(P_{i \to k}^D\right) \tag{17}$$

$$Q_i^G + \sum_{j \in J+} \left(Q_{j \to i}^D\right) = Q_i^C + \sum_{k \in J-} \left(Q_{i \to k}^D\right) \tag{18}$$

$$V_{MIN} < |V_B^{n-t}| < V_{MAX} \tag{19}$$

$$PF_{ESS-MIN} \leqslant PF_{ESS}^{n} \leqslant PF_{ESS-MAX} \tag{20}$$

$$SL^{l-t} < SL_{MAX}^{l} \tag{21}$$

$$\lambda_{ESS}^{n} = \begin{cases} 0, & \textit{if the ESS is active} \\ 1, & \textit{otherwise} \end{cases} \tag{22}$$

$$S_{ESSP}^{n} = \begin{cases} Assign, & if \; \lambda_{ESS}^{n} = 0 \\ 0, & if \; \lambda_{ESS}^{n} = 1 \end{cases} \tag{23}$$

$$S_{ESSQ}^{n} = \begin{cases} Assign, & if \; \lambda_{ESS}^{n} = 0 \\ 0, & if \; \lambda_{ESS}^{n} = 1 \end{cases} \tag{24}$$

$$P_{ESS-MIN} < P_{ESS} < P_{ESS-MAX} \tag{25}$$

$$P^t_{ESS,C} \leq P^t_{ESS} \leq P^t_{ESS,D} \tag{26}$$

$$E_{ESS-MIN} < E_{ESS} < E_{ESS-MAX} \tag{27}$$

where,

- Equations (17) and (18) signify the active and reactive power balance of a bus i [46].
- Equation (19) denotes the voltage constraint of each bus [46].
- Equation (20) ensures that the p.f. on the dispatch of an ESS within the range 0.95 to 1 [77].
- Equation (21) guarantees that the line loading of line l must not surpass the maximum boundary SL^l_{max} to safeguard the thermal stability of cables . The SL^l_{max} is considered as 80% based on industry practices of planning as described in [46].
- Equations (22) to (24) denote the ESS allocation constraints.
- Equations (25) to (27) guarantees that the ESS power or energy must not surpass their maximum limits throughout charging and discharging phases. Additionally, (1) to (7) assure the operation of ESSs within the specified SOC limits [46].

4. FSCABC optimization and proposed approaches

4.1 FSCABC optimization approach

In this paper, the FSCABC algorithm proposed in [66, 67] is applied for optimizing the grid-connected ESS placement problem. The ABC algorithm is proposed by Karaboga in 2005 [69, 78, 79], which is a bio-inspired swarm intelligence metaheuristic search technique. The possibility of being trapped in local optima while using ABC algorithm [66, 67, 71] can be solved by hybridization with two useful approaches: (1) the fitness scaling approach; and (2) the chaotic approach [66, 67].

With the first approach, the raw fitness values are scaled in a range suited to selection function which are used to select the next generations bees with a high probability of selection to bees. This basically converts the raw fitness results (which are returned by the fitness function) to values well-matched to selection function. The chaotic approach enriches the searching behavior of traditional ABC and assists to avoid the trapping possibility into local optimum [66, 67]. Chaos theory is characterized by the well-known butterfly effect ascertained by Lorenz [80]. After searching by each bee of ABC colony, the chaotic search is conducted in the neighborhood of the present best solution which provides a better solution into the subsequent generation phase. With the above considerations, the FSABC is applied for optimizing the proposed ESS placement problem. The overall FSCABC optimization process is clarified by the flow chart as depicted in Fig. 1(a). Among many fitness scaling methods such as linear, rank, power and top scaling, the power and rank scaling

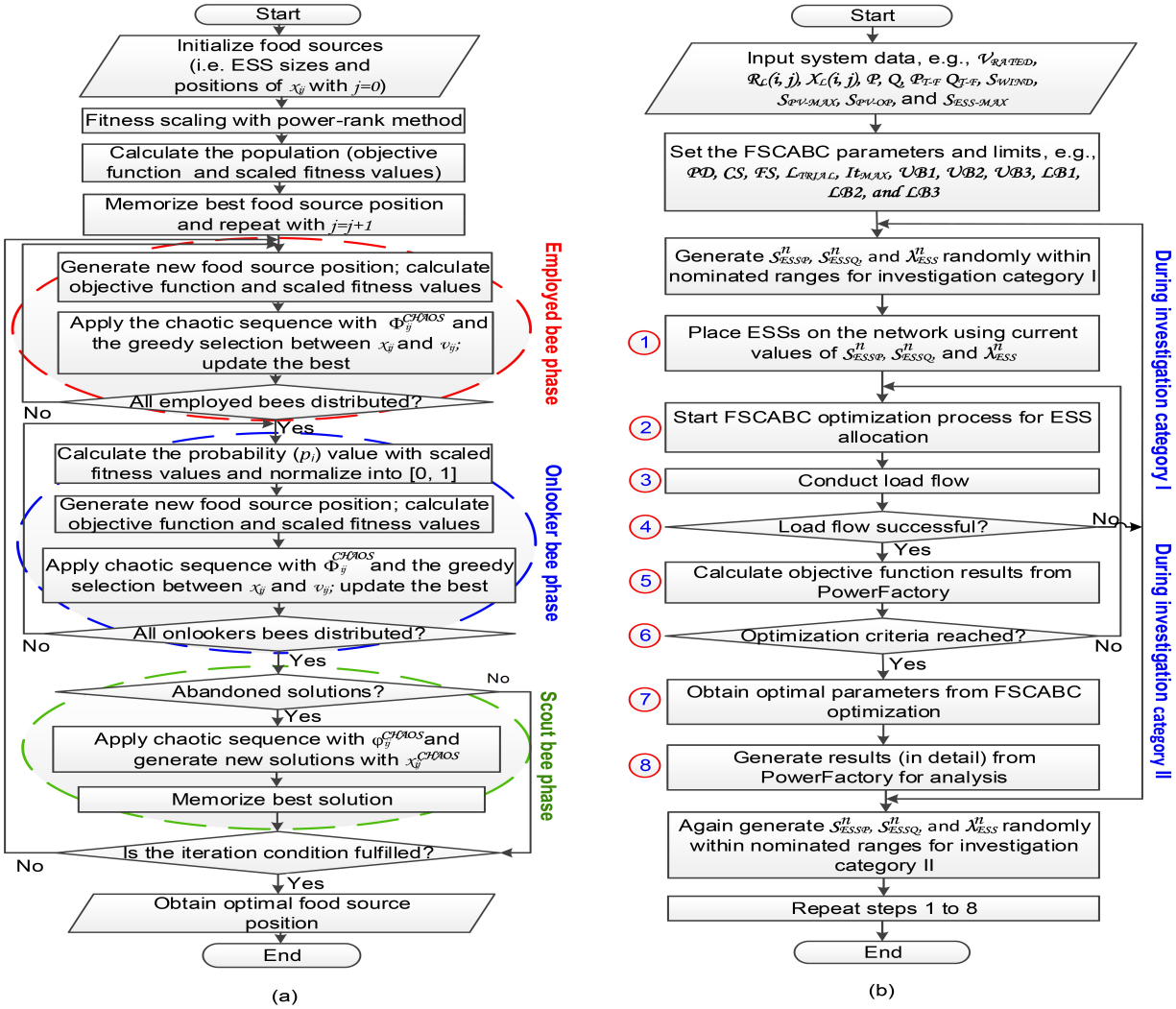

Figure 1: (a) Flowchart of FSCABC optimization approach and (b) flowchart of the proposed optimal ESS allocation approach.

are hybridized to remove their individual limitations. For instance, power scaling can find a solution promptly while having instability problem and rank scaling performs better in terms of stability. Hence, a new power-rank scaling technique, combining both power and rank strategies, is proposed as follows:

$$fit_i^{SCALE} = \frac{r_{a-i}^q}{\sum_{i=1}^{FS} r_{a-i}^q} \tag{28}$$

where, r_{a-i} = the rank of ith bee, FS = the number of food sources, and q = the exponential value for power computation.

According to the chaos theory, minute changes in initial conditions cause widely diverging outcomes, providing long-term behavioural prediction impossible in general [67]. The chaotic

search is defined by the well-known logistic function as given in (29).

$$x_i^{n+1} = \mu^{bif}\, x_i^n\, (1 - x_i^n), \quad i = 1, 2, ..., FS \tag{29}$$

where, x_i^n = the ith chaotic variable, n = the iteration number, and μ^{bif} = the bifurcation parameter of the system with $\mu^{bif} \in [0, 4]$. The chaotic behaviour is exhibited with $\mu^{bif} = 4$, $x_i^0 \in (0, 1)$, and $x_i^0 \notin \{0.25, 0.5, 0.75\}$.

In the initialization phase, the colony size (CS) of solutions $x_{ij} (i = 1, 2, ..., FS;\ j = 1, 2, ..., PD)$ (PD = problem dimension) is determined with the number of employed bees (N_{EmB}) and the number of onlooker bees (N_{OnB}), while satisfying $CS = N_{EmB} + N_{OnB}$. The population is initialized with $j = 0$ as represented in (30).

$$x_{i0} = LB + \psi_{ij}^{rand}\, (UB - LB), \quad i = 1, 2, ..., FS \tag{30}$$

where, LB = the lower boundary, UB = the upper boundary, and ψ_{ij}^{rand} = a random number within the range [0, 1]. By applying the following equation, each employed bee travels from one old position x_{ij} to a new candidate position v_{ij}:

$$v_{ij} = x_{ij} + \Phi_{ij}^{rand}\, (x_{ij} - x_{kj}) \tag{31}$$

In (31), $k \in 1, 2, .., FS$ and $j \in 1, 2, .., PD$ are randomly nominated and k should be different from i, where, Φ_{ij}^{rand} = uniform random number within the range [-1, 1]. If the new position value v_{ij} is better than x_{ij}, then x_{ij} is updated with v_{ij}, otherwise x_{ij} remains unaltered. The probability of a food source (p_i) and the fitness scores of food sources of employed bees (fit^{fs}) are estimated by (32) and (33), respectively, where, $f(x_i)^{obj}$ signifies the values of a objective function to be optimized.

$$p_i = \frac{fit_i^{fs}}{\sum_{j=1}^{FS} fit_j^{fs}} \tag{32}$$

$$fit_i^{fs} = \begin{cases} \frac{1}{1+f(x_i)^{obj}}, & f(x_i)^{obj} \geq 0 \\ 1 + |f(x_i)^{obj}|, & f(x_i)^{obj} < 0 \end{cases} \tag{33}$$

Depending on the p_i value, the onlooker bee chooses a food source by applying a roulette wheel selection approach and then this new location is determined by (34), where ω_i^{EB} = weight coefficient in relation to employed bee information.

$$v_{ij} = x_{ij} + \omega_i^{EB} \Phi_{ij}^{rand}\, (x_{ij} - x_{kj}) \tag{34}$$

As the parameter Φ is the key factor for convergence in ABC [66], the chaotic sequence of this parameter is defined by (35) and applied into (31) & (34).

$$\Phi_{ij}^{CHAOS} = 2 \times \left[4\Phi_{ij}^{rand} \left(1 - \Phi_{ij}^{rand}\right)\right] - 1 \tag{35}$$

The abandoned solutions are improved in the scout bee phase and replaced by a new solution

x_{ij}^{CHAOS} as given in (36).

$$x_{ij}^{CHAOS} = min\left(x_{ij}\right) + \varphi_{ij}^{rand}\left[max\left(x_{ij}\right) - min\left(x_{ij}\right)\right] \tag{36}$$

where, $max(x_{ij}) = max\left\{x_{1j}, x_{2j}, ..., x_{Nj}\right\}$, $min(x_{ij}) = min\left\{x_{1j}, x_{2j}, ..., x_{Nj}\right\}$, and φ_{ij}^{rand} = a random number within the range [-1, 1]. Similar to parameter Φ, the chaotic sequence of φ_{ij}^{rand} is defined by (37) and applied into (36).

$$\varphi_{ij}^{CHAOS} = 4\varphi_{ij}^{rand}\left(1 - \varphi_{ij}^{rand}\right) \tag{37}$$

4.2 Proposed approach

Figure 1(b) represents the proposed methodology for solving the optimal ESS allocation problem. The FSCABC parameters are initialized after entering all the necessary component data in a distribution network. The parameters and variables of FSCABC optimization process are summarized in Table 1. For feeder load scaling, the P_{T-F} & Q_{T-F} are entered to the feeder and a voltage dependency of loads is created. The time-variant characteristics of [46] are applied for characterizing the loads, wind, and solar DGs. Subsequently, the problem is formulated to minimize the sum of C_{VDev}^{n}, C_{LLd}^{l}, C_{PLs}^{l}, and C_{ESS}^{UTo}. The investigations are carried out in two stages: (1) investigation category I− using a uniform ESS size; and (2) investigation category II− using non-uniform ESS sizes.

The ESS locations are determined through the decision variable λ_{ESS}^{n} (can be 0 or 1, while 0 signifies the ESS is active and 1 means inactive). The size of an ESS (MVA) in the network is obtained from the decision variables S_{ESSP}^{n} (MW) and S_{ESSQ}^{n} (MVar). The S_{ESSP}^{n}, S_{ESSQ}^{n}, and λ_{ESS}^{n} are generated randomly within the selected ranges and applied to the system. The S_{ESSP}^{n} and S_{ESSQ}^{n} are injected such that the maximum number of ESSs having lower capacity (in the ranges P = 0.1 MW to 2 MW, Q = 0.1 MVar to 1 MVar for investigation category I and P = 0.1 MW to 2.5 MW, Q = 0.1 MVar to 1 MVar for investigation category II) can be dispersed in the network. During investigation category II, the S_{ESSQ}^{n} is kept uniform for all ESSs on the network, while the S_{ESSP}^{n} is assigned non-uniformly to the ESSs. The initial values are nominated randomly according to the selected ranges of P and Q, and ESS sizes to be tested on the network. The overall nomination of ESS sizes is subject to $LB1$, $UB1$, $LB2$, $UB2$, $LB3$, $UB3$, AC and DC bus sizes, transformer size, string size of ESSs, and inverter specifications. Due to the complexity of the ESS allocation problem, all selected parameters and steps are necessary to find the optimal solution. Finally, the FSCABC optimization process determines the optimal values of S_{ESSP}^{n}, S_{ESSQ}^{n}, and λ_{ESS}^{n} by fulfilling the objective function constraints.

In this paper, a variable p.f. (within the range 0.95 to 1) approach for sizing is applied to the dispatch of ESSs. The intention of the approach is that the ESSs will inject both P and Q rather than injecting P only (the unity p.f. case). This approach improves the performance of the network through more reactive power compensation. Hence, the ESS locations and size are found utilizing the multi-functionality of ESSs in supplying the MW and MVar required to assist the voltage controllers on the network and minimize line loading and losses.

Table 1: Parameters and variables of FSCABC optimization approach

Type	**Parameters/variables**	**Description/settings**
Input parameters	V_{RATED},$R_L(i,j)$, $X_L(i,j)$, P, Q, P_{T-F}, Q_{T-F}, S_{WIND}, S_{PV-MAX}, S_{PV-OP}, and $S_{ESS-MAX}$	Essential for the distribution network model.
Output parameters	C^n_{VDev}, C^l_{LLd}, C^l_{PLs}, and C^{UTo}_{ESS}	Essential for the objective function.
Decision variables	S^n_{ESSP}	This variable represents the amount of P injection from the ESSs in the network.
	S^n_{ESSQ}	This variable represents the amount of Q injection from the ESSs in the network.
	λ^n_{ESS}	This variable represents the position of ESSs in the network.
FSCABC parameters	μ^{bif}, ψ^{rand}_{ij}, Φ^{rand}_{ij}, φ^{rand}_{ij}, and x^0_i	Settings: $\mu^{bif} \in [0,4]$, $\psi^{rand}_{ij} \in [0,1]$, $\Phi^{rand}_{ij} \in [-1,1]$, $\varphi^{rand}_{ij} \in [-1,1]$, $x^0_i \in (0,1)$, and $x^0_i \notin \{0.25, 0.5, 0.75\}$.
	PD, CS, FS, L_{TRIAL}, and It_{MAX}	Settings: $PD = 3$, $CS = 100$, $FS = CS/2$ =population size, $L_{TRIAL} = 60$, and $It_{MAX} = 1000$.
FSCABC bounds	For S^n_{ESSP}: $LB1$ and $UB1$	Settings: $LB1 = 0.1$ MW and $UB1 = 2$ MW for investigation category I; $LB1 = 0.1$ MW and $UB1 = 2.5$ MW for investigation category II.
	For S^n_{ESSQ}: $LB2$ and $UB2$	Settings: $LB2 = 0.1$ MVar and $UB2 = 1$ MVar for both investigation category I and investigation category II.
	For λ^n_{ESS}: $LB3$ and $UB3$	Settings: $LB3 = 0$ and $UB3 = 1$.

5. Testing, factor assignment, and performance indices

This section explores the distribution network used for testing of the proposed approach, the assignment of essential factors, and necessary indices to evaluate the improvements of system performance. The details of the factor assignment and performance measurement can be found in [46].

5.1 Test network

The proposed approach is tested in a distribution system whose single line diagram is illustrated in Fig. 2. This is an IEEE-33 bus distribution network (radial) whose detailed model can be found in [46]. The buses are denoted by numbers (1 to 33) and the lines are indicated by the letter 'L'. Bus 1 is the feeder and lines L33 to L37 are the tie lines of the network [46]. The ESS model (described in Section 2) is allocated distributively throughout the network. A high RES penetration scenario is built by incorporating two wind DGs and seven solar DGs. The loads, wind DGs, and solar DGs are modeled using built-in templates of PowerFactory and applying the data found in [46]. The wind DGs, namely WDG1 and WDG2, are allocated on bus 18 and bus 24, respectively, while the solar DGs- PV1, PV2, PV3, PV4, PV5, PV6, and PV7 are located on bus 5, bus 21, bus 31, bus 8, bus 12, bus 28,

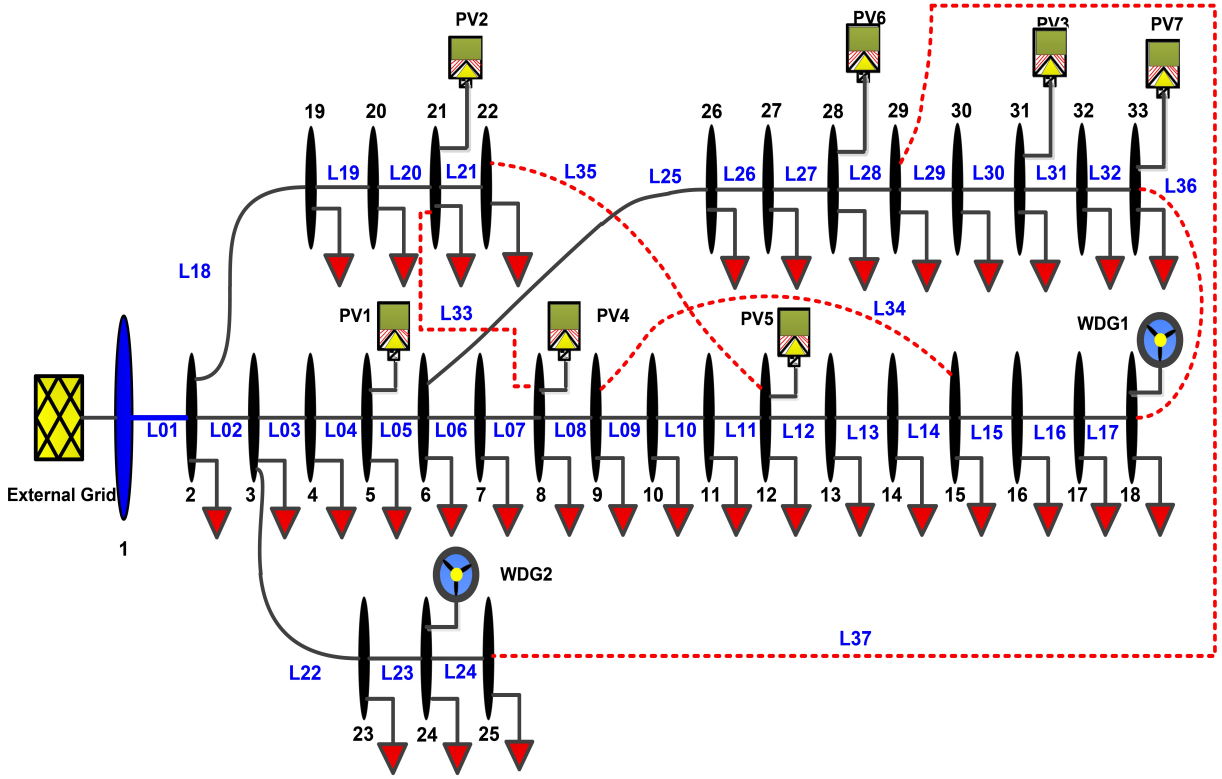

Figure 2: Single-line diagram of the distribution network model.

and bus 33, respectively. The overall system model information is: base MVA = 10 MVA; substation voltage = 12.66 kV; size of WDG1 & WDG2 = 1 MW; size of PV1, PV2, & PV3 = 400 kVA; size of PV4, PV5, PV6, & PV7 = 500 kVA; P_{T-F} = 3.715 MW; Q_{T-F} = 2.3 MVar; and S_{PV-OP}= 85% of S_{PV-MAX} [46].

5.2 Assignment of scaling factors and voltage dependency

The system loads follow the IEEE-RTS model and the loads of the feeder are scaled by following the steps described in [46]. The total real and reactive powers are computed using a scale (Ψ_{SCALE}) and considering the voltage dependency of loads as presented in (38) and (39), respectively [46].

$$P = \Psi_{SCALE} \,.\, P_0 \left[aP \,.\, \left(\frac{V_B^n}{V_{REF}} \right)^{e_{aP}} + bP. \left(\frac{V_B^n}{V_{REF}} \right)^{e_{bP}} + (1 - aP - bP) \,.\, \left(\frac{V_B^n}{V_{REF}} \right)^{e_{cP}} \right] \quad (38)$$

$$Q = \Psi_{SCALE} \,.\, Q_0 \left[aQ \,.\, \left(\frac{V_B^n}{V_{REF}} \right)^{e_{aQ}} + bQ. \left(\frac{V_B^n}{V_{REF}} \right)^{e_{bQ}} + (1 - aQ - bQ) \,.\, \left(\frac{V_B^n}{V_{REF}} \right)^{e_{cQ}} \right] \quad (39)$$

where, $(1 - aP - bP) = cP$ and $(1 - aQ - bQ) = cQ$.

The assigned load coefficients are $aP = aQ = 0.4$, $bP = bQ = 0.3$, and $cP = cQ = 0.3$, and the set exponents are $e_{aP} = e_{aQ} = 0$, $e_{bP} = e_{bQ} = 1$, and $e_{cP} = e_{cQ} = 2$ [46]. The scaling of RES generation (wind and solar DGs) outputs is accomplished as per the characteristics provided in [46]. The investigation is conducted for a time resolution of 24 hours, where the hourly data of loads, solar, and wind are used as the input [46].

5.3 Performance indices of the system

This section derives various performance indices of the system required for performance evaluation. The voltage deviation index is calculated from network buses, while indices for line loading and line losses are estimated from network lines. Further details of these indices in relation to definition and formulation can be found in [46].

5.3.1 Indices for voltage deviation and profile improvement

Considering ±5% deviation limit, the V_{MAX}, V_{MIN}, and voltage deviation for nth bus are calculated. The voltage deviation index ($VDevI$) is expressed as a percentage and defined by (40) [46].

$$\% \; VDevI = \sum_{n=1}^{N} \left(\frac{|V_{RATED} - V_B^n|}{V_{RATED}} \right) \times 100 \tag{40}$$

The voltage profile of nth bus, overall voltage profile, and the voltage profile improvement index of the system are defined by (41), (42), and (43), respectively [46].

$$VProf^n = V_B^n \; S_{Ld}^n \; \Pi^n \tag{41}$$

$$VProf = \sum_{n=1}^{N} VProf^n \tag{42}$$

$$VPII = \frac{VProf_{w-ESS}}{VProf_{wo-ESS}} \tag{43}$$

where,

$$\sum_{i=1}^{N} \Pi^n = 1 \tag{44}$$

5.3.2 Index for line loading

The index for line loading ($LLdI$) represents the measurement of total loading or demand levels of lines, which is defined by (45) [46]. In this study, the percent line loading of lth line, for base case and after ESS placement, is formulated by (46) and (11), respectively [46].

$$LLdI = \frac{\% \; LLdT_{w-ESS}}{\% \; LLdT_{wo-ESS}} = \frac{\sum_{l=1}^{M} \% \; LLd_{ESS}^{l}}{\sum_{l=1}^{M} \% \; LLd_{BASE}^{l}} \tag{45}$$

$$\% \; LLd_{BASE} = \left(\frac{SL^{l}_{BASE}}{SL^{l}_{RATED}} \right) \times 100 \tag{46}$$

5.3.3 Indices for power loss reduction

The indices for the reduction of active, reactive, and total power losses ($PLsRI_P$, $PLsRI_Q$, and $PLsRI_T$) are demarcated by (47), (48), and (49), respectively [46].

$$PLsRI_P = \frac{\sum_{l=1}^{M} P^{l}_{Ls-ESS}}{\sum_{l=1}^{M} P^{l}_{Ls-BASE}} \tag{47}$$

$$PLsRI_Q = \frac{\sum_{l=1}^{M} Q^{l}_{Ls-ESS}}{\sum_{l=1}^{M} Q^{l}_{Ls-BASE}} \tag{48}$$

$$PLsRI_T = \frac{\sum_{l=1}^{M} \sqrt{\left(P^{l}_{Ls-ESS}\right)^2 \; + \; \left(Q^{l}_{Ls-ESS}\right)^2}}{\sum_{l=1}^{M} \sqrt{\left(P^{l}_{Ls-BASE}\right)^2 \; + \; \left(Q^{l}_{Ls-BASE}\right)^2}} \tag{49}$$

6. Results and discussion

This section explores the impact of optimal ESS placement through the PQ injection (on the dispatch of ESSs) to the distribution system. The performance of the system is analyzed in three different case studies: Case 1− without ESS placement (base case), Case 2− ESS placement for a uniform ESS size, and Case 3− ESS placement for non-uniform ESS sizes. Optimal ESS allocation is performed by minimizing the objective function parameters for the same network scenario of [46]. As the ESSs inject P (MW) and Q (MVar) to the network, the p.f. is variable which is limited by $PF_{MIN} = 0.95$ during optimization. The results of the system are summarized in Table 2. The investigation is conducted for a time period of 24 hours and the maximum value of parameters $\%VDevI$, $\%LLdT$, P_{Tot}, and Q_{Tot} for that period is calculated. This section also presents a result comparison between two approaches− the proposed PQ injection approach and the P injection approach of [46]− and reports the performance improvement. The system results using the P injection approach (achieved by [46]) are presented in Table 3, which are categorized as Case 4 and Case 5 for investigation category I and investigation category II, respectively. Similar to [46], the ESS power rating (MVA) is assumed constant over one hour. Furthermore, the system results with different weighting factors in the objective function (8) (using PQ injection approach) are presented in Table 4. In addition, the results obtained from the FSCABC algorithm are compared with the ABC approach and presented in this section.

6.1 Case 1- base case without ESS placement

The reference values of the result parameters such as $\%VDevI$, $\%LLdT$, P_{Tot}, and Q_{Tot} for base case analysis is presented in Table 2. These base values are targeted to minimize

Table 2: Obtained results from the proposed PQ injection approach

P (MW), Q (MVar), and locations of ESSs	$\%VDevI$	$\%LLdT$	P_{Tot} **(MW)**	Q_{Tot} **(MVar)**	**Total ESS Size (MWh)**
Case 1−Without placement of ESSs (base case)					
No ESSs	89.73	269.81	0.11	0.09	-
Case 2−Distributed ESS placement using a uniform ESS size					
ESS9, ESS7, ESS9, ESS14, ESS25, ESS29, ESS30, ESS31, ESS32; for all ESSs P = 0.97 Q= 0.29	67.34	221.85	0.084	0.061	8.11
Case 3−Distributed ESS placement using non-uniform ESS sizes					
ESS7-P=1.19 Q=0.12; ESS10-P=0.72 Q=0.12; ESS14-P=0.80 Q=0.12; ESS16-P=0.37 Q=0.12; ESS17-P=0.37 Q=0.12; ESS22-P=0.37 Q=0.12; ESS25-P=2.5 Q=0.12; ESS29-P=0.72 Q=0.12; ESS30-P=2.5 Q=0.12; ESS31-P=0.37 Q=0.12; ESS32-P=0.69 Q=0.12	66.70	204.38	0.074	0.052	10.67

Table 3: System results with the P injection approach obtained by [46]

P (MW) and locations of ESSs	$\%VDevI$	$\%LLdT$	P_{Tot} **(MW)**	Q_{Tot} **(MVar)**	**Total ESS Size (MWh)**
Case 4−Distributed ESS placement using a uniform ESS size					
ESS9, ESS14, ESS25, ESS28, ESS29, ESS30, ESS31, ESS32, for all ESSs P=0.72 Q=0	75.75	241.13	0.091	0.068	5.79
Case 5−Distributed ESS placement using non-uniform ESS sizes					
ESS8- P=0.34; ESS10- P=0.38; ESS13- P=0.38; ESS16- P=0.82; ESS17- P=0.1; ESS20- P=0.13; ESS22- P=0.1; ESS25- P=2; ESS30- P=1.44; ESS31- P=0.73; ESS32- P=0.78; for all ESSs Q=0	72.16	240.04	0.089	0.067	7.20

Table 4: System results obtained from the PQ injection approach with different weighting factors in (8)

P (MW), Q (MVar), and locations of ESSs	$\%VDevI$	$\%LLdT$	P_{Tot} **(MW)**	Q_{Tot} **(MVar)**	**Total ESS Size (MWh)**
Case 6−Distributed placement using a uniform ESS size $\beta_{VDev} = 0.2$, $\beta_{LLd} = 0.2$, $\beta_{PLs} = 0.3$, and $\beta_{ESS} = 0.3$					
ESS9, ESS14, ESS25, ESS29, ESS30, ESS31, for all ESSs P=1.07 Q=0.33	69.80	226.06	0.083	0.059	6.69
Case 7−Distributed ESS placement using non-uniform ESS sizes $\beta_{VDev} = 0.3$, $\beta_{LLd} = 0.2$, $\beta_{PLs} = 0.3$, and $\beta_{ESS} = 0.2$					
ESS8-P=0.45 Q=0.1; ESS9-P=0.66 Q=0.1; ESS10-P=0.31 Q=0.1; ESS12-P=0.31 Q=0.1; ESS14-P=1.12 Q=0.1; ESS16-P=0.31 Q=0.1; ESS22-P=0.31 Q=0.1; ESS24-P=0.31 Q=0.1; ESS25-P=2.5 Q=0.1; ESS28-P=0.31 Q=0.1; ESS29-P=0.31 Q=0.1; ESS30-P=2.5 Q=0.1; ESS31-P=0.93 Q=0.1; ESS32-P=0.31 Q=0.1; ESS33-P=0.32 Q=0.1	66.39	210.52	0.074	0.051	11.66

through the proposed PQ injection approach of ESSs. Although the V_{Bi} is limited by V_{MAX} and V_{MIN}, the voltage profile can be improved further. Similarly, the line loading and losses can be minimized through the proposed PQ injection approach.

6.2 Case 2- ESS placement using a uniform ESS size

The optimal ESS allocation results for uniform S^n_{ESSP} and S^n_{ESSQ} values (using the PQ injection approach) are presented in Table 2. The S^n_{ESSP}, S^n_{ESSQ}, and λ^n_{ESS} can be identified in Table 2 by the ESS MW (P), ESS MVar (Q), and ESS number, respectively: e.g., for ESS9, P=0.97 and Q=0.29 denote that an ESS of 0.97 MW and 0.29 MVar (total size of 1.01 MVA) is connected to bus 9. Eight ESSs of a uniform size (1.01 MVA) are placed on buses 7, 9, 14, 25, 29, 30, 31, and 32. All the parameters in Case 2 such as $\%VDevI$, $\%LLdT$, P_{Tot}, and Q_{Tot} are minimized compared to Case 1. A noticeable point is that all Case 2 parameters are also minimized compared to Case 4 (tabulated in Table 3). For instance, the values of $\%VDevI$, $\%LLdT$, P_{Tot}, and Q_{Tot} are 75.75%, 241.13%, 0.091 MW, and 0.068 MVar, respectively, while using the P injection approach [46]. In contrast, when using the PQ injection approach, these values are further reduced such as $\%VDevI$=67.34%, $\%LLdT$=221.85%, P_{Tot}=0.084 MW, and Q_{Tot}=0.061 MVar. However, the total ESS size required in Case 2 to improve the performance is 8.11 MWh which is higher than the total ESS size of Case 4 (5.79 MWh). Hence, there is an increase of distribution system investment cost during Case 2 compared to Case 4, while improving the performance better than the Case 4.

6.3 Case 3- ESS placement using non-uniform ESS sizes

After analyzing the impact of optimal ESS placement using non-uniform ESS sizes using the PQ injection approach, the results are summarized in Table 2 as Case 3. In this case study, the S^n_{ESSP} is assigned non-uniformly to all ESSs and the S^n_{ESSQ} is allotted uniformly to all ESSs. The S^n_{ESSP}, S^n_{ESSQ}, and λ^n_{ESS} can be identified in Table 2 by the ESS MW (P), ESS MVar (Q), and ESS number, respectively: e.g., ESS7-P = 1.19 Q=0.12 represents that an ESS of 1.19 MW and 0.12 MVar (total size of 1.03 MVA) is placed to bus 7. Eleven ESSs of non-uniform ESS sizes (as given in Table 2) are placed on buses 7, 10, 14, 16, 17, 22, 25, 29, 30, 31, and 32. It is apparent that all the parameters ($\%VDevI$, $\%LLdT$, P_{Tot}, and Q_{Tot}) are further minimized compared to Case 2. It is also obvious that all Case 3 parameters are minimized compared to Case 5 (given in Table 3). For example, when using the P injection approach, the values of $\%VDevI$, $\%LLdT$, P_{Tot}, and Q_{Tot} are 72.16%, 240.04%, 0.089 MW, and 0.067 MVar, respectively [46]. On the contrary, these values are further reduced while using the PQ injection approach such as $\%VDevI$=66.70%, $\%LLdT$=204.38%, P_{Tot}=0.074 MW, and Q_{Tot}=0.052 MVar. However, for Case 3, the required total ESS size is 10.67 MWh, which signifies an increment in distribution system investment cost over Case 2 (7.43 MWh) and Case 5 (7.20 MWh). This is mainly due to the fact that non-uniform ESS sizing approach (Case 3) is more adjustable in relation to overcoming network operational constraints compared to uniform ESS sizing method (Case 2) and can achieve more optimal performance across the whole network.

6.4 System results with different weighting factors in the objective function

The system results of Table 4 are obtained through the application of PQ injection approach, while using different weighting factors in the objective function (8). This analysis is conducted to apply a trade-off among weighting factors and comprehend the variability of obtained results compared to Case 2 and Case 3, while giving different importance to each performance indicators of (8). The weighting factors are chosen within the range 0 to 1, while their summation is equal to 1. The results are categorized in two case studies such as Case 6 and Case 7 for ESS allocation using a uniform ESS size and non-uniform ESS sizes, respectively. During Case 6, the weighting factors are chosen as $\beta_{VDev} = 0.2$, $\beta_{LLd} = 0.2$, $\beta_{PLs} = 0.3$, and $\beta_{ESS} = 0.3$, while for Case 7 they are set to $\beta_{VDev} = 0.3$, $\beta_{LLd} = 0.2$, $\beta_{PLs} = 0.3$, and $\beta_{ESS} = 0.2$. It is apparent from the analysis of Table 4 that the values of weighting factors impact the results as compared to Case 2 and Case 3. For instance, the values of $\%VDevI$, $\%LLdT$, P_{Tot}, Q_{Tot}, and total ESS size for Case 6 are 69.80%, 226.06%, 0.083 MW, 0.059 MVar, and 6.69 MWh, respectively, where the variability of obtained results are observed as per corresponding parameter values of Case 2. Similar variability is noticed for parameter values during Case 7, while comparing corresponding parameter values of Case 3.

6.5 Overall result analysis and comparison using the PQ injection approach

6.5.1 Comparison in relation to voltage profiles

The voltage profiles using the PQ injection approach for Case 1, Case 2, and Case 3 are depicted in Fig. 3. The feeder voltage profiles for Case 2 and Case 3 (p.u. voltage vs km)

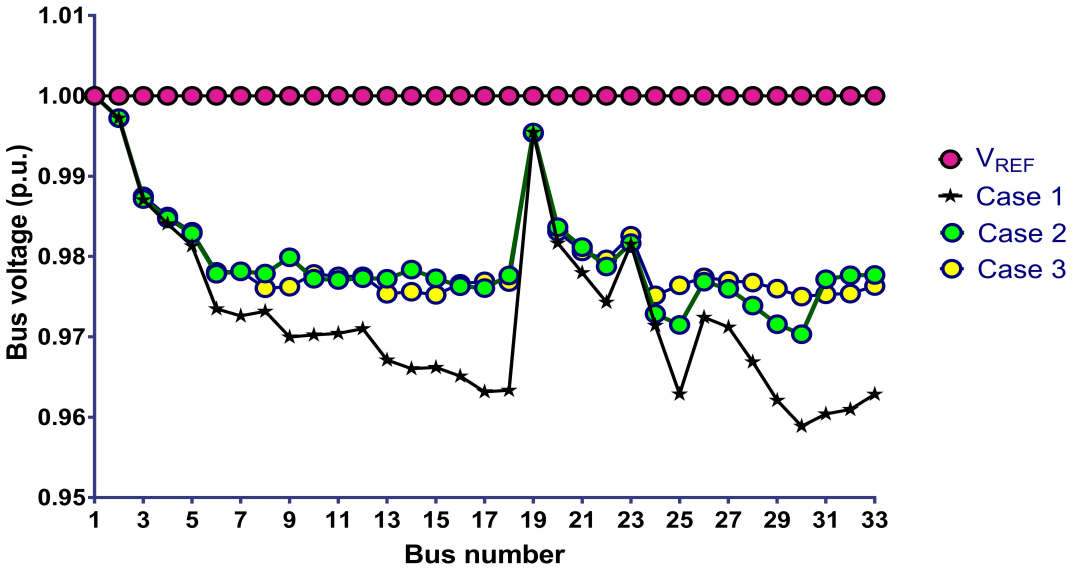

Figure 3: Voltage profiles for various cases using the PQ injection approach.

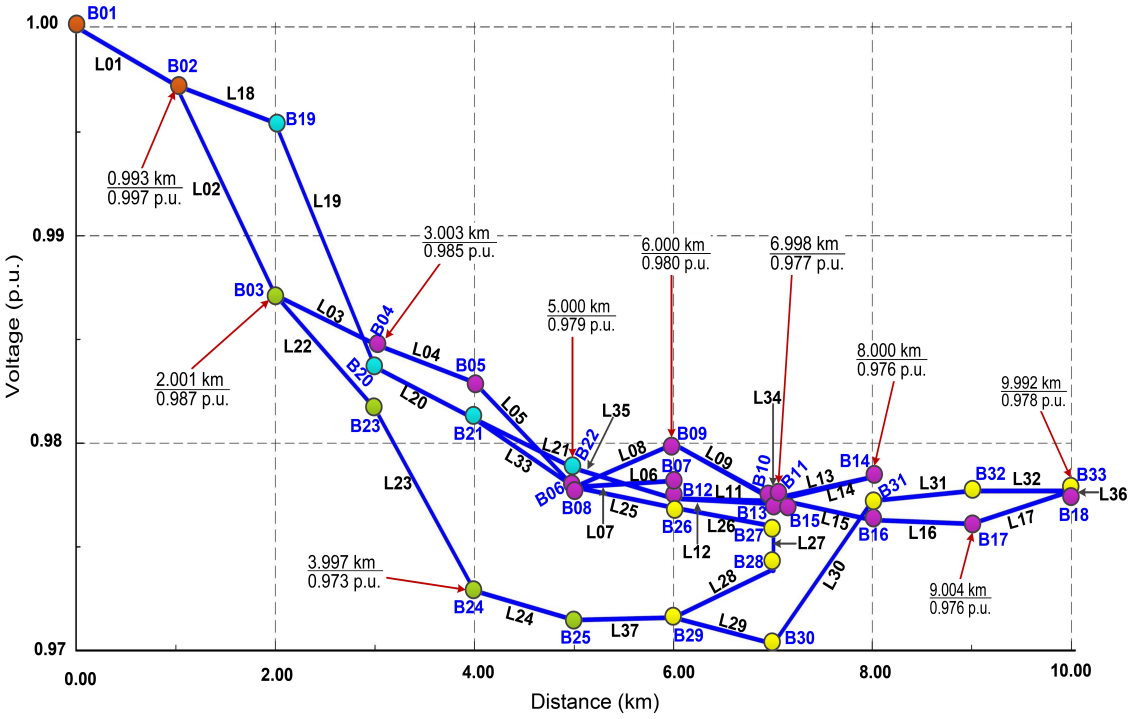

Figure 4: The feeder voltage profile for case 2 using the PQ injection approach.

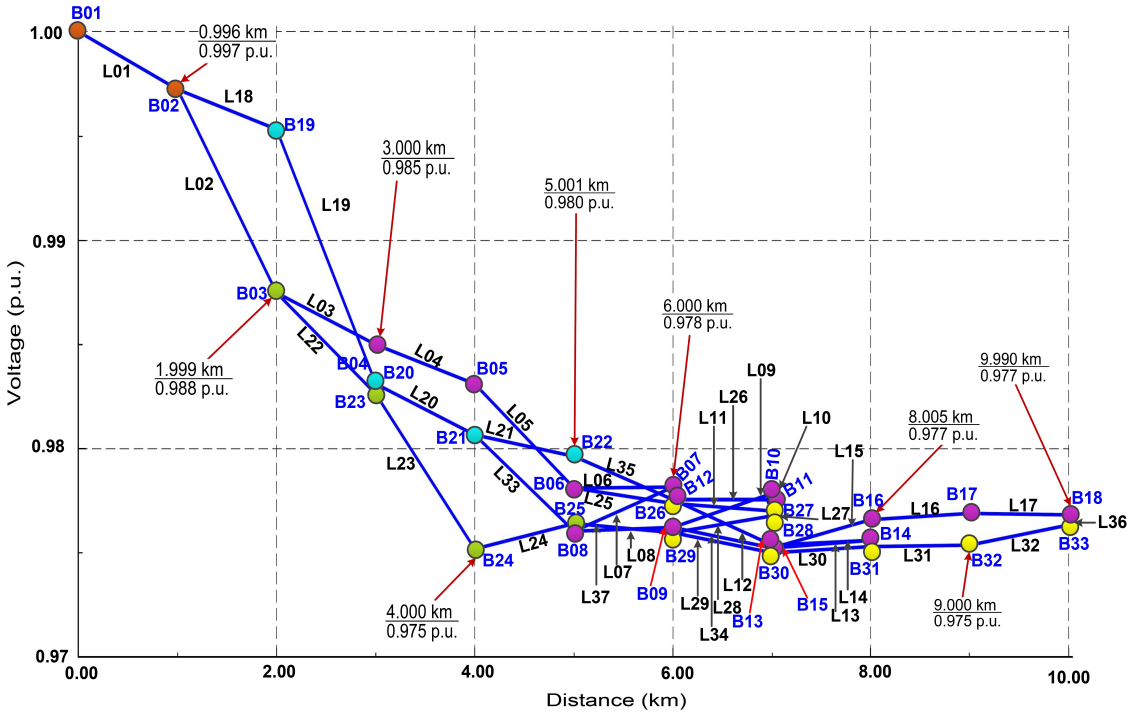

Figure 5: The feeder voltage profile for case 3 using the PQ injection approach.

are illustrated in Fig. 4 and Fig. 5, respectively. Various sections of feeder voltage profiles

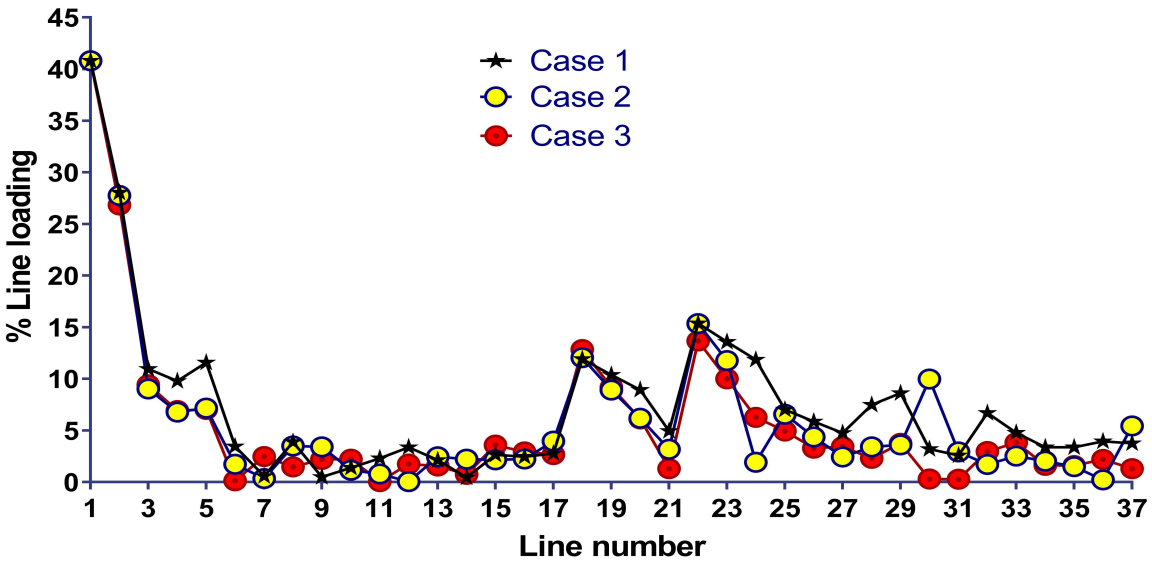

Figure 6: The percent line loading for various cases using the PQ injection approach.

(in terms of feeder length) are indicated with different colors, where all the lines of the feeder have the same length (1km). Although both Case 2 and Case 3 have similar voltage profiles, Case 3 has improvements in the voltage profile at some buses as illustrated in Fig. 3. For instance, according to Fig. 3, Fig. 4, and Fig. 5, Case 3 has improved the bus voltage at bus 24 (Case 3=0.97 p.u., Case 2=0.98 p.u.) and bus 25 (Case 3=0.97 p.u., Case 2=0.98 p.u.) compared to Case 2. Similarly, the voltages are improved for Case 3 at buses 10, 22, 23, and 26 to 30 compared to Case 2. However, Case 2 has improved bus voltage characteristics at buses 7 to 9, 13 to 15, and 31 to 33 compared to Case 3. Figure 4 and Fig. 5 shows that the voltage drop in the feeder section L02-L22-L23-L24-L37-L29-L30 and L16-L17 is higher for Case 2, while Case 3 has higher voltage drops in sections L02-L22-L23-L24 and L08-L29-L30-L31-L32. The highest voltage drop for Case 2 and Case 3 is observed at bus 30 (0.97 p.u.) and bus 24 (0.974 p.u.), respectively. For both Case 2 and Case 3, lower voltage drops occur at buses 2 and 19. From the illustrations, it is evident that both Case 2 and Case 3 have good voltage profiles, where Case 3 ($\%VDevI$=66.70) provides a slightly better voltage profile than Case 2 ($\%VDevI$=67.34).

6.5.2 Comparison in relation to line loading

Figure 6 compares the percent line loadings of Case 1, Case 2, and Case 3, which implies that the loading of each line for all cases is below the maximum boundary 80%. It can be noted that L1 has a maximum loading of 40.80% for all cases, while L2 has about 28% loading for Case 1, 27.76 % for Case 2, and 26.86 % for Case 3. All other lines for Case 2 and Case 3 are lightly loaded (e.g., below 15%). From the viewpoint of line to line loading variation, the line loadings of Case 2 are higher at lines L2, L5-L6, L8-L9, L11, L13-L14, L17, L21-L23, L25-L26, L28-L31, L34-L35, and L37 compared to Case 3. In contrast, Case 3 provides higher loading values at lines L3, L7, L10, L15-L16, L18, L24, L27, L22-L29, L32-

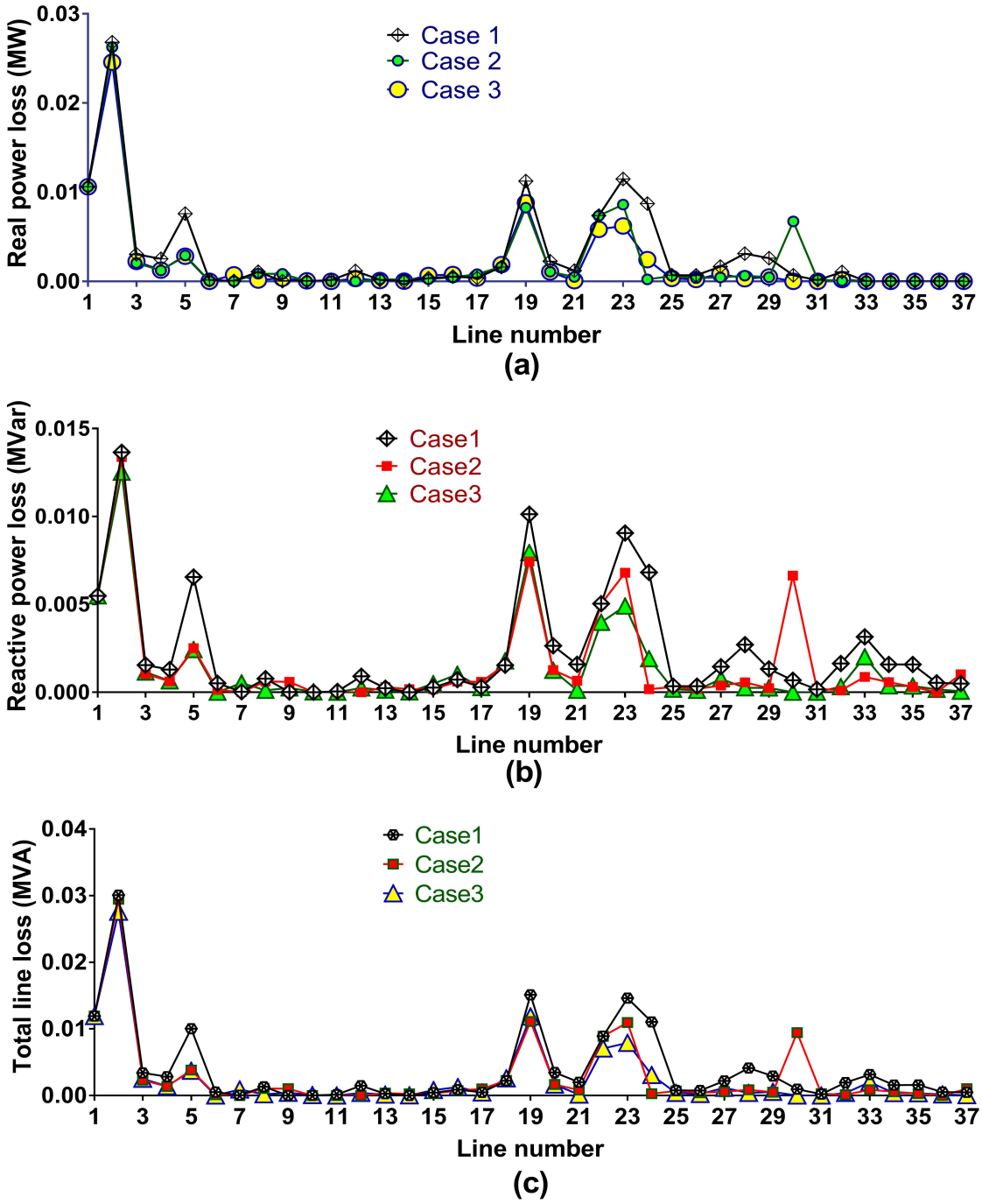

Figure 7: Comparison of losses for various cases using the PQ injection approach (a) active power loss, (b) reactive power loss, and (c) total line loss.

L33, and L36 than Case 2. Overall, Case 3 ($\%LLdT$=204.38) provides better line loadings than Case 2 ($\%LLdT$=221.85). It is apparent from the line loading characteristics of Case 2 and Case 3 that the feeder has sufficient spare capacity to get back from the unexpected situation during outage.

6.5.3 Comparison in relation to line losses

Figure 7 compares the active, reactive, and total power losses of various lines for Case 2 and Case 3 over Case 1. According to Fig. 7(a), L2 has the highest active power loss of 0.026 MW and 0.025 MW for Case 2 and Case 3, respectively. Case 2 has a higher active power loss at lines L2, L4-L5, L7-L9,L13-L14, L17, L21-L23, L25-L26, L28, and L30, while a higher active power loss value is observed at lines L3, L7, L12, L15-L16, L19, L24, and L27 for Case 3. As referred to in Fig. 7(b), again L2 has the highest reactive power loss of 0.013 MVar for both Case 2 and Case 3. Besides, the reactive power loss and total line loss profiles for Case 2 and Case 3 at various lines is almost similar to the real power loss characteristics of Fig. 7(a) except the tie lines. Both Case 2 and Case 3 have reactive power losses in tie lines as depicted in Fig. 7(b). Overall, the losses are little bit higher for Case 2 (e.g., P_{Tot}=0.084, and Q_{Tot}=0.061) compared to Case 3 (e.g., P_{Tot}=0.074, and Q_{Tot}=0.052).

6.5.4 Statistical analysis of FSCABC approach with ABC algorithm

The ABC algorithm is employed for ESS allocation in [46]. The same ABC approach is utilized to verify the results found from the proposed FSCABC technique using the same settings of PD, CS, FS, L_{TRIAL}, It_{MAX}, and bounds as listed in Table 1. Both the FSCABC and the ABC optimization are executed 30 times and the best, worst, and mean objective function values for investigation category I and investigation category II are compared in Table 5. In addition, the standard deviations for FSCABC and ABC algorithms (σ_{FSCABC} and σ_{ABC}) of objective function values are calculated. The lesser value of standard deviation implies smaller deviation among solutions of 30 optimization runs. Table 5 suggests that the solutions obtained from both algorithms (in relation to objective function costs) are very close to each other. It is also evident that more optimal solutions are achieved from the FSCABC approach for both investigation categories. Therefore, it is apparent from the statistical analysis (presented in Table 5) that the proposed FSCABC technique is successful in attaining required optimal solutions of the problem for both investigation categories.

The computer configuration used for simulation is: Intel(R) Xeon 3.5 GHz processor, 64-bit windows 10, and 16 GB RAM. Figure 8 illustrates the convergence test characteristics of FSCABC and ABC optimization approaches for two investigation phases. The convergence results including computation time are tabulated in Table 6. Table 6 implies that the FSCABC algorithm converges after 182 and 274 iterations for investigation category I and investigation category II, respectively. In contrast, the ABC-based approach converges after 257 and 396 iterations for investigation category I and investigation category II, respectively. In other words, the FSCABC-based approach converges faster than the ABC algorithm. The proposed optimization approach is an offline method, where no real time decisions needed to be taken to determine the locations and sizes of ESSs in the network. The focus of

Table 5: Optimization results of FSCABC and ABC for 30 runs

Optimization statistics	**ESS real & reactive powers and locations**	**%VDevI**	**%LLdT**	P_{Tot} (MW)	Q_{Tot} (MVar)	**Total ESS size (MWh)**	**Objective function value ($)**
Distributed ESS placement using a uniform ESS size							
FSCABC best	ESS7, ESS9, ESS14, ESS25, ESS29, ESS30, ESS31, ESS32; for all ESSs P = 0.971 Q= 0.291	67.34	221.85	0.084	0.061	8.11	3730325.40
FSCABC worst	ESS7, ESS9, ESS13, ESS25, ESS29, ESS30, ESS31, ESS32; for all ESSs P = 0.973 Q= 0.311	67.19	224.95	0.085	0.062	8.17	3759149.03
FSCABC mean	ESS7, ESS9, ESS13, ESS25, ESS29, ESS30, ESS31, ESS32; for all ESSs P = 0.967 Q= 0.316	67.19	224.73	0.085	0.062	8.14	3743969.01
σ_{FSCABC}							10434.43
ABC best	ESS7, ESS9, ESS13, ESS25, ESS29, ESS30, ESS31, ESS32; for all ESSs P = 0.965 Q= 0.316	67.23	224.70	0.085	0.062	8.12	3736609.01
ABC worst	ESS7, ESS9, ESS13, ESS25, ESS29, ESS30, ESS31, ESS32; for all ESSs P = 0.974 Q= 0.319	67.02	224.75	0.085	0.062	8.20	3771569.00
ABC mean	ESS7, ESS9, ESS13, ESS25, ESS29, ESS30, ESS31, ESS32; for all ESSs P = 0.969 Q= 0.318	67.12	224.70	0.085	0.062	8.16	3753168.99
σ_{ABC}							13311.39

Table 5 continues

Optimization statistics	ESS real & reactive powers and locations	%VDevI	%LLdT	P_{Tot} (MW)	Q_{Tot} (MVar)	Total ESS size (MWh)	Objective function value ($)
Distributed ESS placement using non-uniform ESS sizes							
FSCABC best	ESS7-P=1.191 Q=0.12; ESS10-P=0.715 Q=0.12; ESS14-P=0.798 Q=0.12; ESS16-P=0.368 Q=0.12; ESS17-P=0.368 Q=0.12; ESS22-P=0.368 Q=0.12; ESS25-P=2.5 Q=0.12; ESS29-P=0.715 Q=0.12; ESS30-P=2.5 Q=0.12; ESS31-P=0.368 Q=0.12; ESS32-P=0.693 Q=0.12	66.70	204.38	0.074	0.052	10.67	4906385.04
FSCABC worst	ESS7-P=1.256 Q=0.12; ESS10-P=0.689 Q=0.12; ESS14-P=0.779 Q=0.12; ESS16-P=0.368 Q=0.12; ESS17-P=0.368 Q=0.12; ESS22-P=0.368 Q=0.12; ESS25-P=2.5 Q=0.12; ESS29-P=0.877 Q=0.12; ESS30-P=2.5 Q=0.12; ESS31-P=0.368 Q=0.12; ESS32-P=0.657 Q=0.12	67.07	204.94	0.074	0.052	10.82	4977685.12
FSCABC mean	ESS7-P=0.885 Q=0.15; ESS8-P=0.488 Q=0.15; ESS9-P=0.460 Q=0.15; ESS11-P=0.460 Q=0.15; ESS13-P=0.809 Q=0.15; ESS16-P=0.460 Q=0.15; ESS25-P=2.372 Q=0.15; ESS29-P=0.460 Q=0.15; ESS30-P=2.5 Q=0.15; ESS31-P=0.460 Q=0.15; ESS32-P=0.815 Q=0.15	66.91	204.69	0.074	0.051	10.74	4939044.94
σ_{FSCABC}							16717.36
ABC best	ESS7-P=0.885 Q=0.15; ESS8-P=0.488 Q=0.15; ESS9-P=0.460 Q=0.15; ESS11-P=0.460 Q=0.15; ESS13-P=0.808 Q=0.15; ESS16-P=0.460 Q=0.15; ESS25-P=2.368 Q=0.15; ESS29-P=0.460 Q=0.15; ESS30-P=2.5 Q=0.15; ESS31-P=0.460 Q=0.15; ESS32-P=0.814 Q=0.15	67.06	204.66	0.074	0.051	10.67	4910064.96
ABC worst	ESS7-P=1.449 Q=0.16; ESS10-P=0.490 Q=0.16; ESS14-P=0.962 Q=0.16; ESS15-P=0.490 Q=0.16; ESS18-P=0.490 Q=0.16; ESS25-P=2.355 Q=0.16; ESS27-P=0.490 Q=0.16; ESS28-P=0.490 Q=0.16; ESS30-P=2.5 Q=0.16; ESS31-P=0.490 Q=0.16; ESS32-P=0.496 Q=0.16	67.33	207.86	0.077	0.056	10.85	4989186.45
ABC mean	ESS7-P=0.882 Q=0.15; ESS8-P=0.491 Q=0.15; ESS9-P=0.460 Q=0.15; ESS11-P=0.460 Q=0.15; ESS13-P=0.809 Q=0.15; ESS16-P=0.460 Q=0.15; ESS25-P=2.369 Q=0.15; ESS29-P=0.460 Q=0.15; ESS30-P=2.5 Q=0.15; ESS31-P=0.460 Q=0.15; ESS32-P=0.814 Q=0.15	67.07	205.02	0.074	0.051	10.75	4945024.96
σ_{ABC}							21751.51

Table 6: Convergence and computation time of FSCABC and ABC algorithms

Investigation category	**FSCABC convergence**	**FSCABC computation time (s)**	**ABC convergence**	**ABC computation time (s)**
I	After 182 iterations	310	After 257 iterations	548
II	After 274 iterations	492	After 396 iterations	762

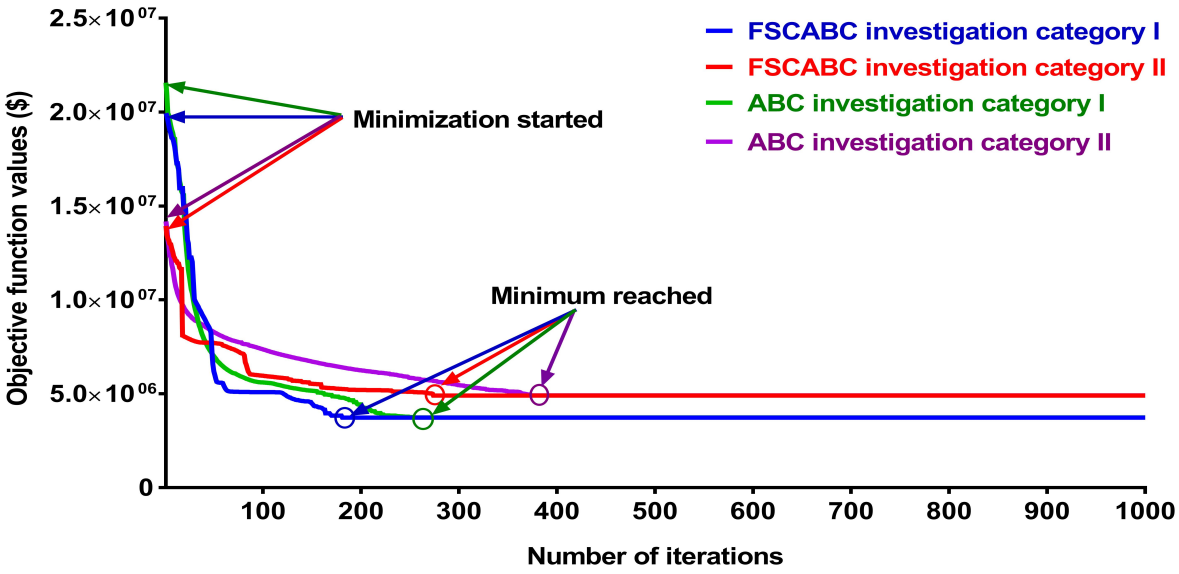

Figure 8: Convergence of FSCABC and ABC algorithms.

the approach is obtaining accurate optimal solutions with acceptable computation costs. However, the searching speed is considered to demonstrate the success of applying proposed FSCABC approach and compare its convergence characteristics or computation time with traditional ABC algorithm. Regarding computation time, FSCABC and ABC approaches take about 310 s and 548 s, respectively, to locate the ESSs during investigation category I. For investigation category II, the FSCABC and ABC algorithms require around 492 s and 762 s, respectively, to allocate the ESSs on the distribution network.

6.6 Overall performance and ESS cost comparison using PQ and P injection approaches

Table 7 represents the performance indices of the system which are evaluated as per Section 5.3. Generally, $VPII > 1$ implies that the system has a good voltage profile. On the contrary, the higher values of $LLdI$, $PLsRI_P$, $PLsRI_Q$, and $PLsRI_T$ signify higher line loading, active power loss, reactive power loss, and total line loss, respectively.

The voltage profile improvement in terms of bus voltage, using the PQ injection approach over the P injection approach for investigation category I and investigation category II, is

Table 7: Performance indices for various cases of Table 2 and Table 3

Case Details	$\boldsymbol{VPII}$	$\boldsymbol{LLdI}$	$\boldsymbol{PLsRI_P}$	$\boldsymbol{PLsRI_Q}$	$\boldsymbol{PLsRI_T}$
Case 1	-	-	-	-	-
For a uniform ESS size					
Case 2	1.08	0.82	0.77	0.71	0.74
Case 4	1.04	0.83	0.80	0.82	0.89
For non-uniform ESS sizes					
Case 3	1.08	0.76	0.68	0.61	0.65
Case 5	1.06	0.82	0.78	0.80	0.89

compared in Fig. 9(a) and Fig. 9(b), respectively. These suggest that the voltage profiles are improved for both investigation categories while using the PQ injection approach. From the viewpoint of point to point bus voltage measurement, the PQ injection approach provides improved voltage profiles at most of the buses for both investigation categories compared to the P injection approach. For instance, the voltage profile improvement is remarkable at buses 4 to 18, 20 to 22, 25 to 27, and 29 to 33 while using the PQ injection approach for investigation category I. For investigation category II, significant improvement in bus voltages is achieved through the PQ injection approach at buses 4 to 7, 9 to 18, and 22 to 31. The overall $VPII$ is improved with the use of the PQ injection approach compared to the P injection approach for both investigation categories as evaluated in Table 7. For instance, the $VPII = 1.04$ for Case 4 (using the P injection approach) is improved to 1.08 during Case 2 (using the PQ injection approach) under investigation category I. On the other hand, Case 3 provides $VPII = 1.08$ which is higher than Case 5 ($VPII = 1.06$) during investigation category II.

Figure 10(a) and Fig. 10(b) compare the line loading characteristics using the PQ injection approach over the P injection approach for investigation category I and investigation category II, respectively. These suggest that the line loading during the PQ injection approach is minimized for both investigation categories compared to the P injection approach. The opposite characteristics are observed at some points on the curves such as at L9-L10, L13-L14, L22, L25-L26, and L30 for investigation category I and at L9-L10, L18, L24-L27, and L36 for investigation category II. The line loading minimization using the PQ injection approach is also realized from the $LLdI$ value tabulated in Table 7. During investigation category I, the PQ injection approach provides $LLdI = 0.82$ (Case 2) which is 0.83 (Case 4) while using the P injection approach. On the other hand, the $LLdI$ provided by the P injection approach is 0.81 (Case 5) which is minimized to 0.76 (Case 3) with the use of the PQ injection approach for investigation category II.

Figure 11 and Fig. 12 compare the active, reactive, and total line losses using the PQ injection and the P injection approaches for investigation category I and investigation category II, respectively. According to these illustrations, for both investigation categories, the PQ injection approach minimizes the real, reactive, and total line losses at most of the

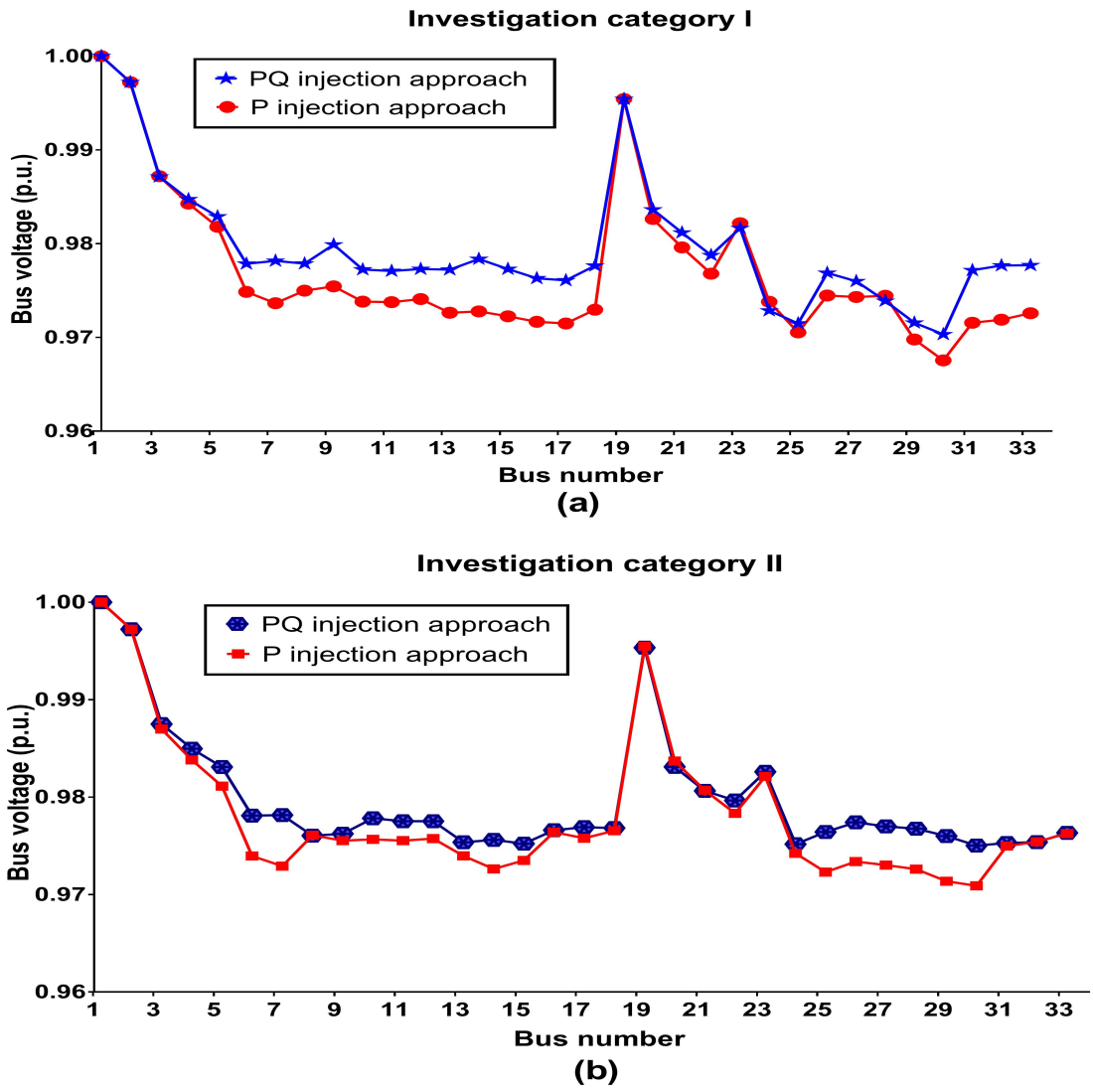

Figure 9: Voltage profile comparison in terms of bus voltage using PQ and P injection approaches– (a) voltage profile comparison for investigation category I and (b) voltage profile comparison for investigation category II.

lines compared to the P injection approach. For both investigation categories in Fig. 11, although P injection approach minimizes losses at very few lines, the losses are minimized at most of the lines by the PQ injection approach. For example, the P injection approach provides lower amounts of active, reactive, and total line losses compared to the PQ injection approach at lines L2, L9, L22-L23, and L30 for investigation category I, while the PQ injection approach minimizes more losses at other lines over the P injection approach. During investigation category II, the PQ injection approach minimizes higher amounts of active, reactive, and total line losses compared to the P injection approach at most of the lines except L9, L16, L18-L19, L22, L24, and L27. These minimization characteristics are also summarized in Table 7 as loss minimization indices which exhibit that Case 2 minimizes

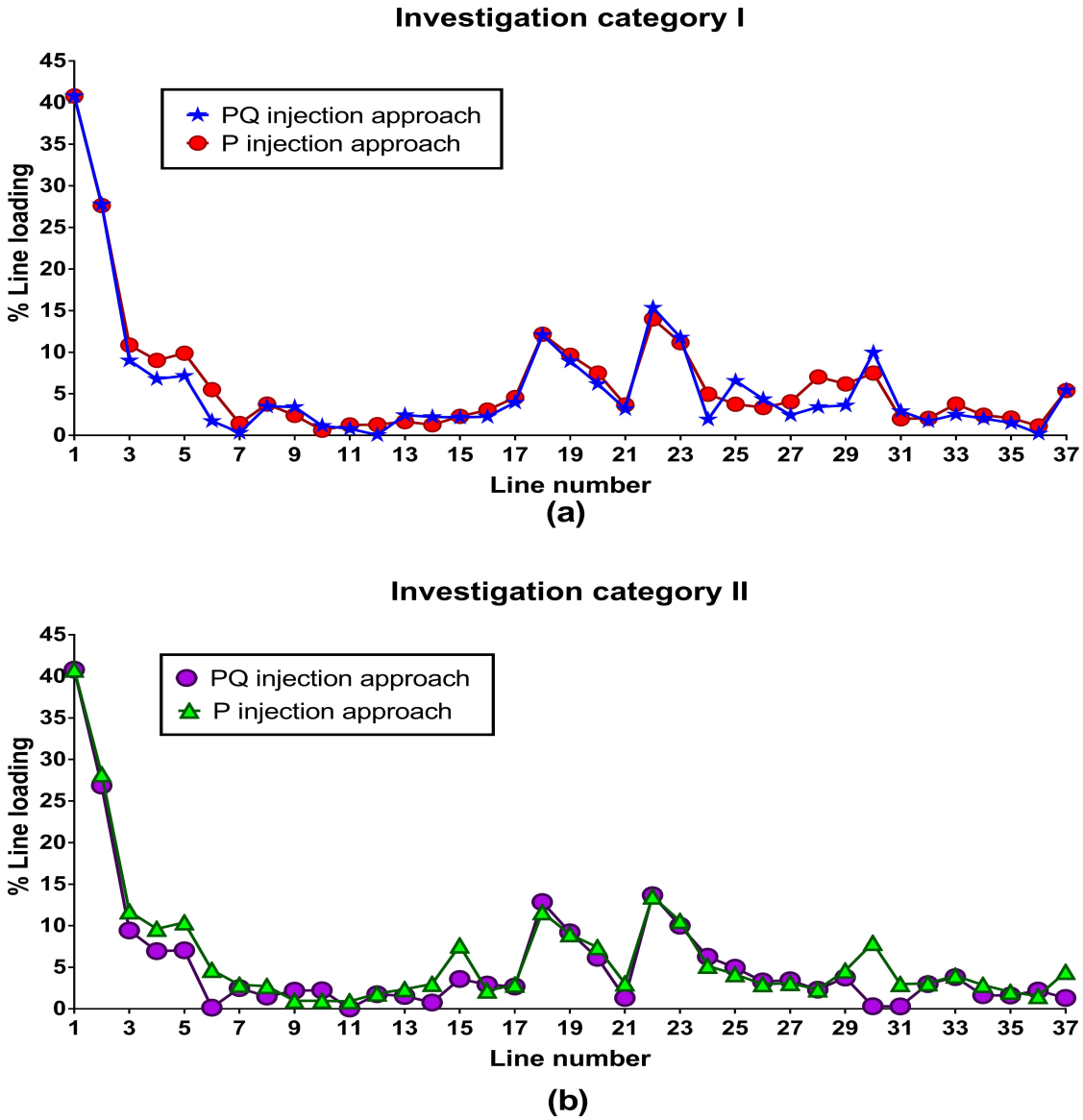

Figure 10: Comparison of %line loading using PQ and P injection approaches– (a) line loading comparison for investigation category I and (b) line loading comparison for investigation category II.

higher amount of active, reactive, and total line losses compared to Case 4, while Case 3 delivers lower amount of losses over Case 5.

The overall performance improvement (expressed in percentage), using the PQ injection approach over the P injection approach, is estimated in Table 8. This suggests that the PQ injection approach achieves 11.11% improvement for voltage deviation, 8% for line loading, 7.18% for active power loss, 11.13% for reactive power loss, and 8.59% for total line loss over the P injection approach during investigation category I. On the contrary, during investigation category II, the proposed PQ approach attains 7.56% improvement for voltage deviation, 14.86% for line loading, 17.45% for active power loss, 21.77% for reactive power

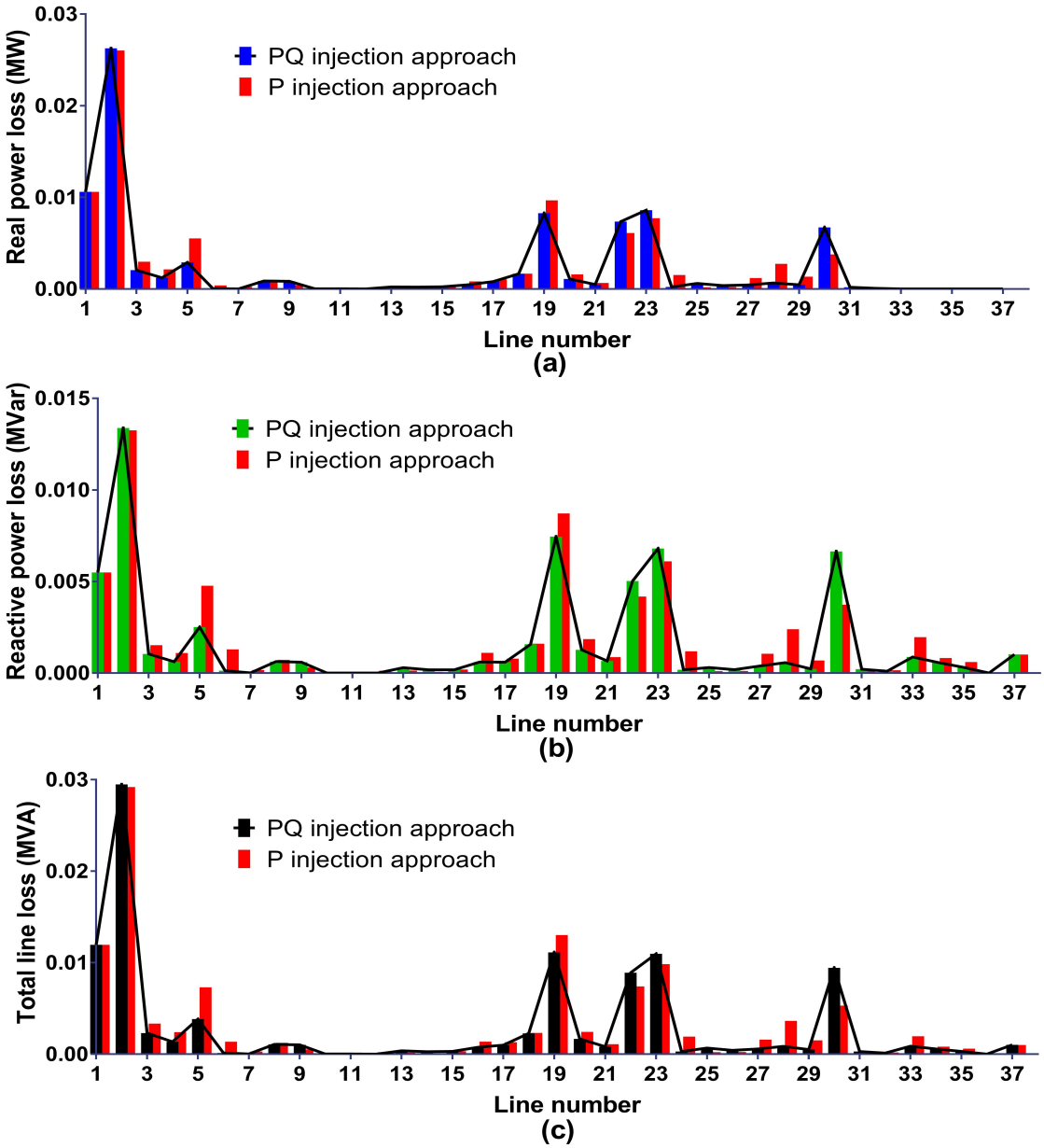

Figure 11: Comparison of losses using PQ and P injection approaches for investigation category I– (a) comparison of active power loss, (b) comparison of reactive power loss, and (c) comparison of total line loss.

loss, and 18.97% for total line loss compared to the P injection approach. The overall comparison in terms of performance indices and total ESS unit cost is presented in Fig. 13. It is evident from the characteristics that the proposed PQ injection approach achieves higher performance improvement compared to the P injection approach for both investigation categories. However, the PQ injection approach requires higher distribution network investment cost, and the amount is higher for investigation category II than investigation category I.

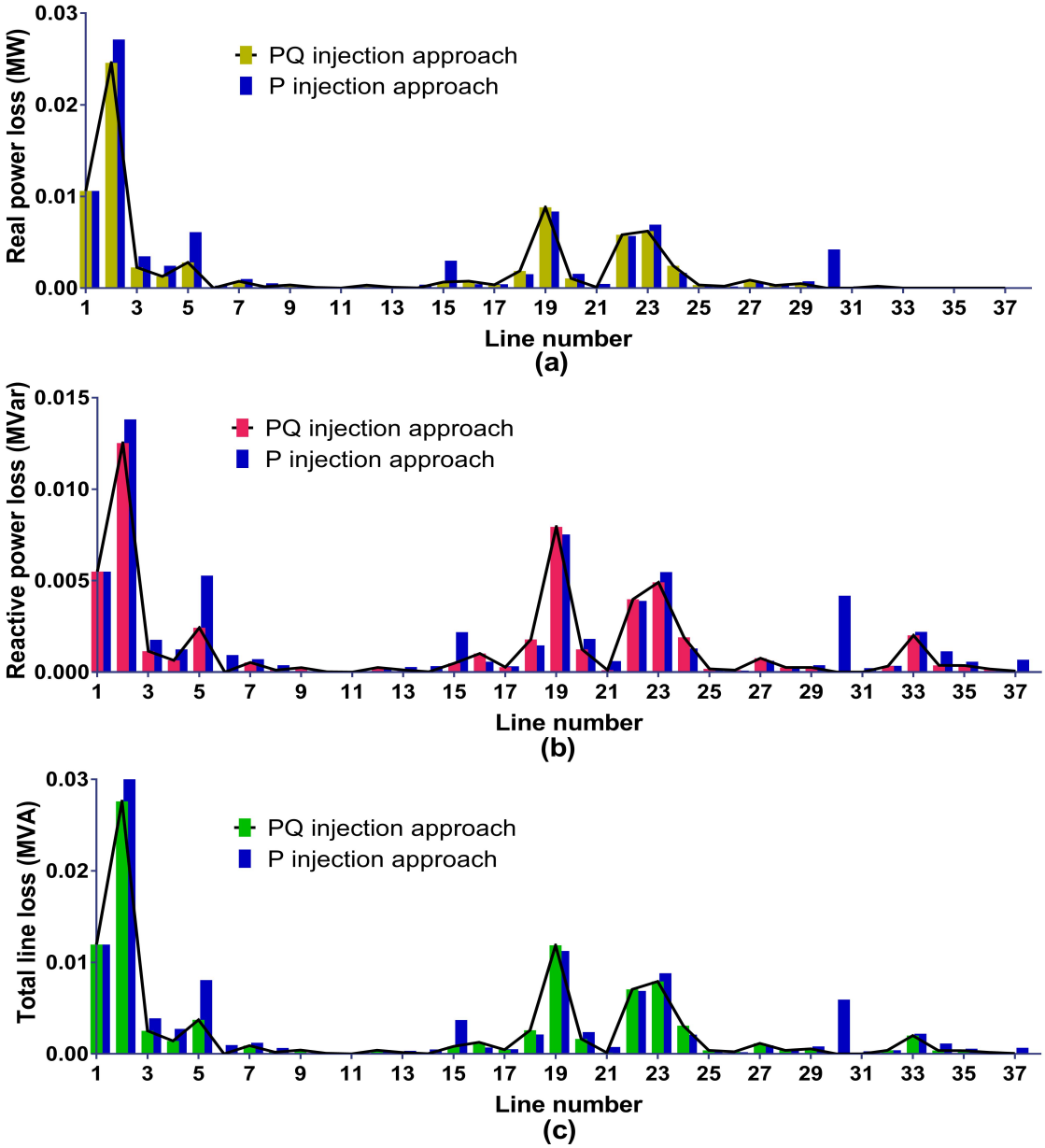

Figure 12: Comparison of losses using PQ and P injection approaches for investigation category II– (a) comparison of active power loss, (b) comparison of reactive power loss, and (c) comparison of total line loss.

Table 8: Performance improvement using the PQ injection approach compared to the P injection approach

Evaluation parameters	P injection approach	PQ injection approach	Improvement
For a uniform ESS size			
$\%VDevI$	75.75	67.34	11.11%
$\%LLdT$	241.13	221.85	8%
$P_{Tot}(MW)$	0.091	0.084	7.18%
$Q_{Tot}(MVar)$	0.068	0.061	11.13%
Total line loss (MVA)	0.113	0.104	8.59%
For non-uniform ESS sizes			
$\%VDevI$	72.16	66.70	7.56%
$\%LLdT$	240.04	204.38	14.86%
$P_{Tot}(MW)$	0.089	0.074	17.45%
$Q_{Tot}(MVar)$	0.067	0.052	21.77%
Total line loss (MVA)	0.112	0.090	18.97%

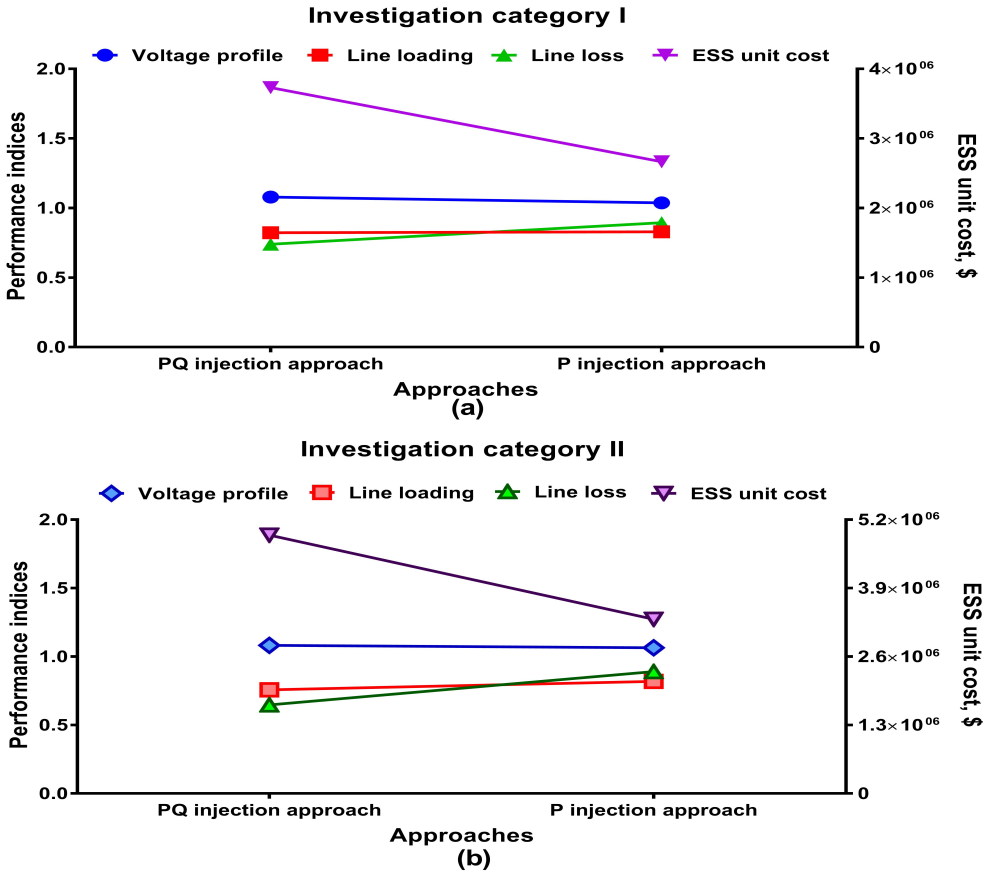

Figure 13: Performance and ESS cost comparison for various cases– (a) for investigation category I (b) for investigation category II.

7. Conclusions

This paper has presented an effective strategy to allocate the distributed ESSs in distribution systems applying the FSCABC hybrid meta-heuristic optimization approach. The system performance is improved significantly by minimizing some key problems of distribution networks such as voltage deviation, power losses, and line loading through the application of the PQ injection approach. The obtained results from the FSCABC technique are verified by applying the ABC algorithm. Related indices are calculated to measure the performance improvement and a performance comparison of PQ injection and P injection approaches is presented. The following conclusions can be made based on the investigations carried out in this paper:

- The PQ injection approach successfully achieves 11.11% and 7.56% improvements in minimizing voltage deviation over the P injection approach for a uniform ESS size and non-uniform ESS sizes, respectively.
- For a uniform ESS size, the proposed PQ injection approach also achieves improvements in minimizing line loading and total line loss over the P injection approach by 8% and 8.59%, respectively. On the other hand, during non-uniform ESS size investigation, 14.86% improvement in line loading minimization and 18.97% improvement in total line loss reduction are achieved by the PQ injection approach compared to the P injection approach.
- The proposed PQ injection approach improves the network performances through increasing the distribution system investment cost. Hence, a tradeoff in relation to performance expectations and costs should be made.

Regarding future works, a sensitivity analysis regarding the optimal ESS allocation, optimal operation of ESSs taking into account RES uncertainty and the impact on ESS lifetime, detailed analysis regarding cost or financial impacts of the obtained ESS sizes, ESS placement targeting power quality improvement, and inclusive ESS sizing can be investigated. Furthermore, the performance and accuracy of the ESS allocation and sizing problem may be improved by formulating the problem as a multi-objective function.

Acknowledgment

This research is supported by an Australian Government Research Training Program (RTP) scholarship and Edith Cowan University (ECU)−Australia. We gratefully acknowledge the technical assistance and support of Mr Wayne Ong of DIgSILENT Pacific, Melbourne, Australia, and Mr Peter Willis of DIgSILENT Pacific, Perth, Australia. We also thankfully acknowledge all support provided by DIgSILENT GmbH, Gomaringen, Germany.

References

[1] C. Bussar, P. Stöcker, Z. Cai, L. Moraes Jr, D. Magnor, P. Wiernes, N. van Bracht, A. Moser, D. U. Sauer, Large-scale integration of renewable energies and impact on storage demand in a European renewable power system of 2050–Sensitivity study, Journal of Energy Storage 6 (2016) 1–10.

[2] C. K. Das, M. A. Ehsan, M. A. Kader, M. J. Alam, G. M. Shafiullah, A practical biogas based energy neutral home system for rural communities of Bangladesh, Journal of Renewable and Sustainable Energy 8 (2) (2016) 023101.

[3] C. K. Das, M. A. Kader, M. J. Alam, Design and implementation of a hybrid energy neutral home system for Bangladesh, International Journal of Renewable Energy Resources 3 (2) (2017) 66–72.

[4] C. K. Das, M. J. Alam, An innovative energy neutral home system for rural areas of Bangladesh, in: Electrical & Computer Engineering (ICECE), 7th International Conference on, IEEE, 2012, pp. 888–891.

[5] K. P. Kumar, B. Saravanan, Day ahead scheduling of generation and storage in a microgrid considering demand side management, Journal of Energy Storage 21 (2019) 78–86.

[6] N. Mousavi, G. Kothapalli, D. Habibi, M. Khiadani, C. K. Das, An improved mathematical model for a pumped hydro storage system considering electrical, mechanical, and hydraulic losses, Applied Energy 247 (2019) 228–236.

[7] S. M. Hossain, C. K. Das, M. S. Hossan, S. Jarin, Electricity from wasted energy of the moving vehicle using speed breaker, Jurnal Teknologi (Sciences & Engineering) 73:1 (2015) 129–134.

[8] C. K. Das, S. M. Hossain, M. S. Hossan, Introducing speed breaker as a power generation unit for minor needs, in: Informatics, Electronics & Vision (ICIEV), International Conference on, IEEE, 2013, pp. 1–6.

[9] J. Song, W. Yang, Y. Higano, X. Wang, Introducing renewable energy and industrial restructuring to reduce GHG emission: Application of a dynamic simulation model, Energy conversion and management 96 (2015) 625–636.

[10] P. Mazumder, M. H. Jamil, C. K. Das, M. A. Matin, Hybrid energy optimization: An ultimate solution to the power crisis of St. Martin Island, Bangladesh, in: 9th International Forum on Strategic Technology (IFOST), 2014, pp. 363–368.

[11] P. Ariyaratna, K. M. Muttaqi, D. Sutanto, A novel control strategy to mitigate slow and fast fluctuations of the voltage profile at common coupling point of rooftop solar PV unit with an integrated hybrid energy storage system, Journal of Energy Storage 20 (2018) 409–417.

[12] T. A. Short, Distribution reliability and power quality, CRC Press, 2005.

[13] P. Härtel, M. Doering, M. Jentsch, C. Pape, K. Burges, R. Kuwahata, Cost assessment of storage options in a region with a high share of network congestions, Journal of Energy Storage 8 (2016) 358–367.

[14] M. Zamani-Gargari, F. Kalavani, M. Abapour, B. Mohammadi-Ivatloo, Reliability assessment of generating systems containing wind power and air separation unit with cryogenic energy storage, Journal of Energy Storage 16 (2018) 116–124.

[15] M. Islam, A. M. S. Alam, C. K. Das, Multi-agent system modeling for managing limited distributed generation of microgrid, in: 2nd International Conference on Electrical Information and Communication Technologies (EICT), 2015, pp. 533–538.

[16] E. G. Carrano, F. G. Guimarães, R. H. C. Takahashi, O. M. Neto, F. Campelo, Electric distribution network expansion under load-evolution uncertainty using an immune system inspired algorithm, IEEE Transactions on Power Systems 22 (2) (2007) 851–861.

[17] C. K. Das, O. Bass, G. Kothapalli, T. S. Mahmoud, D. Habibi, Overview of energy storage systems in distribution networks: Placement, sizing, operation, and power quality, Renewable and Sustainable Energy Reviews 91 (2018) 1205 – 1230.

[18] L. A. Wong, V. K. Ramachandaramurthy, P. Taylor, J. Ekanayake, S. L. Walker, S. Padmanaban, Review on the optimal placement, sizing and control of an energy storage system in the distribution network, Journal of Energy Storage 21 (2019) 489–504.

[19] I. Kim, A case study on the effect of storage systems on a distribution network enhanced by high-capacity photovoltaic systems, Journal of Energy Storage 12 (2017) 121–131.

[20] T. Bocklisch, Hybrid energy storage approach for renewable energy applications, Journal of Energy Storage 8 (2016) 311–319.

[21] F. Cebulla, T. Naegler, M. Pohl, Electrical energy storage in highly renewable European energy systems: Capacity requirements, spatial distribution, and storage dispatch, Journal of Energy Storage 14 (2017) 211–223.

[22] O. D. Montoya, A. Garces, G. Espinosa-Perez, A generalized passivity-based control approach for power compensation in distribution systems using electrical energy storage systems, Journal of Energy Storage 16 (2018) 259–268.

[23] O. D. Montoya, W. Gil-González, A. Garces, G. Espinosa-Perez, Indirect IDA-PBC for active and reactive power support in distribution networks using SMES systems with PWM-CSC, Journal of Energy Storage 17 (2018) 261–271.

[24] A. Marini, M. A. Latify, M. S. Ghazizadeh, A. Salemnia, Long-term chronological load modeling in power system studies with energy storage systems, Applied Energy 156 (2015) 436–448.

[25] A. J. Pimm, T. T. Cockerill, P. G. Taylor, The potential for peak shaving on low voltage distribution networks using electricity storage, Journal of Energy Storage 16 (2018) 231–242.

[26] D. Parra, S. A. Norman, G. S. Walker, M. Gillott, Optimum community energy storage system for demand load shifting, Applied Energy 174 (2016) 130–143.

[27] H. L. Ferreira, R. Garde, G. Fulli, W. Kling, J. P. Lopes, Characterisation of electrical energy storage technologies, Energy 53 (2013) 288–298.

[28] R. Moreno, R. Moreira, G. Strbac, A MILP model for optimising multi-service portfolios of distributed energy storage, Applied Energy 137 (2015) 554–566.

[29] T. Thien, D. Schweer, D. vom Stein, A. Moser, D. U. Sauer, Real-world operating strategy and sensitivity analysis of frequency containment reserve provision with battery energy storage systems in the German market, Journal of Energy Storage 13 (2017) 143–163.

[30] M. Bahramipanah, R. Cherkaoui, M. Paolone, Decentralized voltage control of clustered active distribution network by means of energy storage systems, Electric Power Systems Research 136 (2016) 370–382.

[31] M. Nick, R. Cherkaoui, M. Paolone, Optimal allocation of dispersed energy storage systems in active distribution networks for energy balance and grid support, IEEE Transactions on Power Systems 29 (5) (2014) 2300–2310.

[32] M. Nick, R. Cherkaoui, M. Paolone, Optimal siting and sizing of distributed energy storage systems via alternating direction method of multipliers, International Journal of Electrical Power & Energy Systems 72 (2015) 33–39.

[33] D. Parra, M. Gillott, S. A. Norman, G. S. Walker, Optimum community energy storage system for PV energy time-shift, Applied Energy 137 (2015) 576–587.

[34] Y. Li, B. Feng, G. Li, J. Qi, D. Zhao, Y. Mu, Optimal distributed generation planning in active distribution networks considering integration of energy storage, Applied Energy 210 (2018) 1073–1081.

[35] C. Brivio, S. Mandelli, M. Merlo, Battery energy storage system for primary control reserve and energy arbitrage, Sustainable Energy, Grids and Networks 6 (2016) 152–165.

[36] J. Fleer, P. Stenzel, Impact analysis of different operation strategies for battery energy storage systems providing primary control reserve, Journal of Energy Storage 8 (2016) 320–338.

[37] J. Fleer, S. Zurmühlen, J. Meyer, J. Badeda, P. Stenzel, J.-F. Hake, D. U. Sauer, Techno-economic evaluation of battery energy storage systems on the primary control reserve market under consideration of price trends and bidding strategies, Journal of Energy Storage 17 (2018) 345–356.

[38] J. Sardi, N. Mithulananthan, M. Gallagher, D. Q. Hung, Multiple community energy storage planning in distribution networks using a cost-benefit analysis, Applied Energy 190 (2017) 453–463.

[39] G. Merei, C. Berger, D. U. Sauer, Optimization of an off-grid hybrid PV–Wind–Diesel system with different battery technologies using genetic algorithm, Solar Energy 97 (2013) 460–473.

[40] I. Staffell, M. Rustomji, Maximising the value of electricity storage, Journal of Energy Storage 8 (2016) 212 – 225.

[41] A. Ogunjuyigbe, T. Ayodele, O. Akinola, Optimal allocation and sizing of PV/Wind/Split-diesel/Battery hybrid energy system for minimizing life cycle cost, carbon emission and dump energy of remote residential building, Applied Energy 171 (2016) 153–171.

[42] F. J. De Sisternes, J. D. Jenkins, A. Botterud, The value of energy storage in decarbonizing the electricity sector, Applied Energy 175 (2016) 368–379.

[43] A. S. A. Awad, T. H. M. El-Fouly, M. M. A. Salama, Optimal ESS allocation and load shedding for improving distribution system reliability, IEEE Transactions on Smart Grid 5 (5) (2014) 2339–2349.

[44] A. V. Pombo, J. Murta-Pina, V. F. Pires, Multiobjective formulation of the integration of storage systems within distribution networks for improving reliability, Electric Power Systems Research 148 (2017) 87–96.

[45] J. Xiao, Z. Zhang, L. Bai, H. Liang, Determination of the optimal installation site and capacity of battery energy storage system in distribution network integrated with distributed generation, IET Generation, Transmission & Distribution 10 (3) (2016) 601–607.

[46] C. K. Das, O. Bass, G. Kothapalli, T. S. Mahmoud, D. Habibi, Optimal placement of distributed energy storage systems in distribution networks using artificial bee colony algorithm, Applied Energy 232 (2018) 212 – 228.

[47] S. Wen, H. Lan, Q. Fu, C. Y. David, L. Zhang, Economic allocation for energy storage system considering wind power distribution, IEEE Transactions on Power Systems 30 (2) (2015) 644–652.

[48] K. Mahani, F. Farzan, M. A. Jafari, Network-aware approach for energy storage planning and control in the network with high penetration of renewables, Applied Energy 195 (2017) 974–990.

[49] Y. Zheng, D. J. Hill, Z. Y. Dong, Multi-agent optimal allocation of energy storage systems in distribution systems, IEEE Transactions on Sustainable Energy 8 (4) (2017) 1715–1725.

[50] Y. Zheng, Z. Y. Dong, F. J. Luo, K. Meng, J. Qiu, K. P. Wong, Optimal allocation of energy storage system for risk mitigation of DISCOs with high renewable penetrations, IEEE Transactions on Power Systems 29 (1) (2014) 212–220.

[51] Y. Tang, S. H. Low, Optimal placement of energy storage in distribution networks, IEEE Transactions on Smart Grid 8 (6) (2017) 3094–3103.

[52] M. Motalleb, E. Reihani, R. Ghorbani, Optimal placement and sizing of the storage supporting transmission and distribution networks, Renewable Energy 94 (2016) 651–659.

[53] T. Yunusov, D. Frame, W. Holderbaum, B. Potter, The impact of location and type on the performance of low-voltage network connected battery energy storage systems, Applied Energy 165 (2016) 202–213.

[54] M. G. Ippolito, M. L. Di Silvestre, E. R. Sanseverino, G. Zizzo, G. Graditi, Multi-objective optimized management of electrical energy storage systems in an islanded network with renewable energy sources under different design scenarios, Energy 64 (2014) 648–662.

[55] V. Jani, H. Abdi, Optimal allocation of energy storage systems considering wind power uncertainty, Journal of Energy Storage 20 (2018) 244–253.

[56] A. S. A. Awad, T. H. M. El-Fouly, M. M. A. Salama, Optimal ESS allocation for load management application, IEEE Transactions on Power Systems 30 (1) (2015) 327–336.

[57] N. Jayasekara, M. A. S. Masoum, P. J. Wolfs, Optimal operation of distributed energy storage systems to improve distribution network load and generation hosting capability, IEEE Transactions on Sustainable Energy 7 (1) (2016) 250–261.

[58] A. Giannitrapani, S. Paoletti, A. Vicino, D. Zarrilli, Optimal allocation of energy storage systems for voltage control in LV distribution networks, IEEE Transactions on Smart Grid 8 (6) (2017) 2859–2870.

[59] A. Crossland, D. Jones, N. Wade, Planning the location and rating of distributed energy storage in LV networks using a genetic algorithm with simulated annealing, International Journal of Electrical Power & Energy Systems 59 (2014) 103–110.

[60] O. Babacan, W. Torre, J. Kleissl, Siting and sizing of distributed energy storage to mitigate voltage impact by solar PV in distribution systems, Solar Energy 146 (2017) 199–208.

[61] A. S. A. Awad, T. H. M. EL-Fouly, M. M. A. Salama, Optimal ESS allocation for benefit maximization in distribution networks, IEEE Transactions on Smart Grid 8 (4) (2017) 1668–1678.

[62] H. Saber, M. Moeini-Aghtaie, M. Ehsan, Developing a multi-objective framework for expansion planning studies of distributed energy storage systems (DESSs), Energy 157 (2018) 1079–1089.

[63] Y. M. Atwa, E. F. El-Saadany, Optimal allocation of ESS in distribution systems with a high penetration of wind energy, IEEE Transactions on Power Systems 25 (4) (2010) 1815–1822.

[64] P. Prakash, D. K. Khatod, Optimal sizing and siting techniques for distributed generation in distribution systems: A review, Renewable and Sustainable Energy Reviews 57 (2016) 111–130.

[65] M. D. Al-Falahi, S. Jayasinghe, H. Enshaei, A review on recent size optimization methodologies for standalone solar and wind hybrid renewable energy system, Energy Conversion and Management 143 (2017) 252–274.

[66] C. K. Das, O. Bass, T. S. Mahmoud, G. Kothapalli, N. Mousavi, D. Habibi, M. A. Masoum, Optimal allocation of distributed energy storage systems to improve performance and power quality of distribution networks, Applied Energy 252 (2019) 113468.

[67] Y. Zhang, L. Wu, Weights optimization of FNN by scaled chaotic ABC algorithm, International Journal of Digital Content Technology & its Applications 6 (2012) 13.

[68] D. Karaboga, B. Basturk, A powerful and efficient algorithm for numerical function optimization: Artificial bee colony (ABC) algorithm, Journal of Global Optimization 39 (3) (2007) 459–471.

[69] F. S. Abu-Mouti, M. E. El-Hawary, Optimal distributed generation allocation and sizing in distribution systems via artificial bee colony algorithm, IEEE Transactions on Power Delivery 26 (4) (2011) 2090–2101.

[70] D. Karaboga, B. Basturk, On the performance of artificial bee colony (ABC) algorithm, Applied Soft Computing 8 (1) (2008) 687–697.

[71] G. Zhu, S. Kwong, Gbest-guided artificial bee colony algorithm for numerical function optimization, Applied Mathematics and Computation 217 (7) (2010) 3166–3173.

[72] S. Rothgang, T. Baumhöfer, H. van Hoek, T. Lange, R. W. De Doncker, D. U. Sauer, Modular battery design for reliable, flexible and multi-technology energy storage systems, Applied Energy 137 (2015) 931–937.

[73] E. Rodrigues, R. Godina, J. Catalo, Modelling electrochemical energy storage devices in insular power network applications supported on real data, Applied Energy 188 (2017) 315 – 329.

[74] B. K. Das, Y. M. Al-Abdeli, G. Kothapalli, Effect of load following strategies, hardware, and thermal load distribution on stand-alone hybrid CCHP systems, Applied energy 220 (2018) 735–753.

[75] 2017-18 Synergy electricity price increases. synergy, australia. [Online]. Available: https://www.infiniteenergy.com.au/2017-18-synergy-electricity-price-increases/. [accessed 17 october 2017].

[76] D. Rastler, Electricity energy storage technology options–A white paper primer on applications, costs, and benefits, Tech. rep., Electric Power Research Institute (December 2010).

[77] Western Power, Technical rules-reactive power capability, section 3.3.3.1 (Perth Western Australia, 23 December 2011).

[78] D. Karaboga, An idea based on honey bee swarm for numerical optimization, Tech. rep., Technical report-tr06, Erciyes University, Engineering Faculty, Computer Engineering Department (2005).

[79] L. dos Santos Coelho, P. Alotto, Gaussian artificial bee colony algorithm approach applied to Loney's solenoid benchmark problem, IEEE Transactions on Magnetics 47 (5) (2011) 1326–1329.

[80] A. S. Elwakil, S. Ozoguz, M. P. Kennedy, Creation of a complex butterfly attractor using a novel lorenz-type system, IEEE Transactions on Circuits and Systems I: Fundamental Theory and Applications 49 (4) (2002) 527–530.